UCRL-ID-121265

WEXFORD
Containment Data Report

T. Stubbs
R. Heinle

May 1995

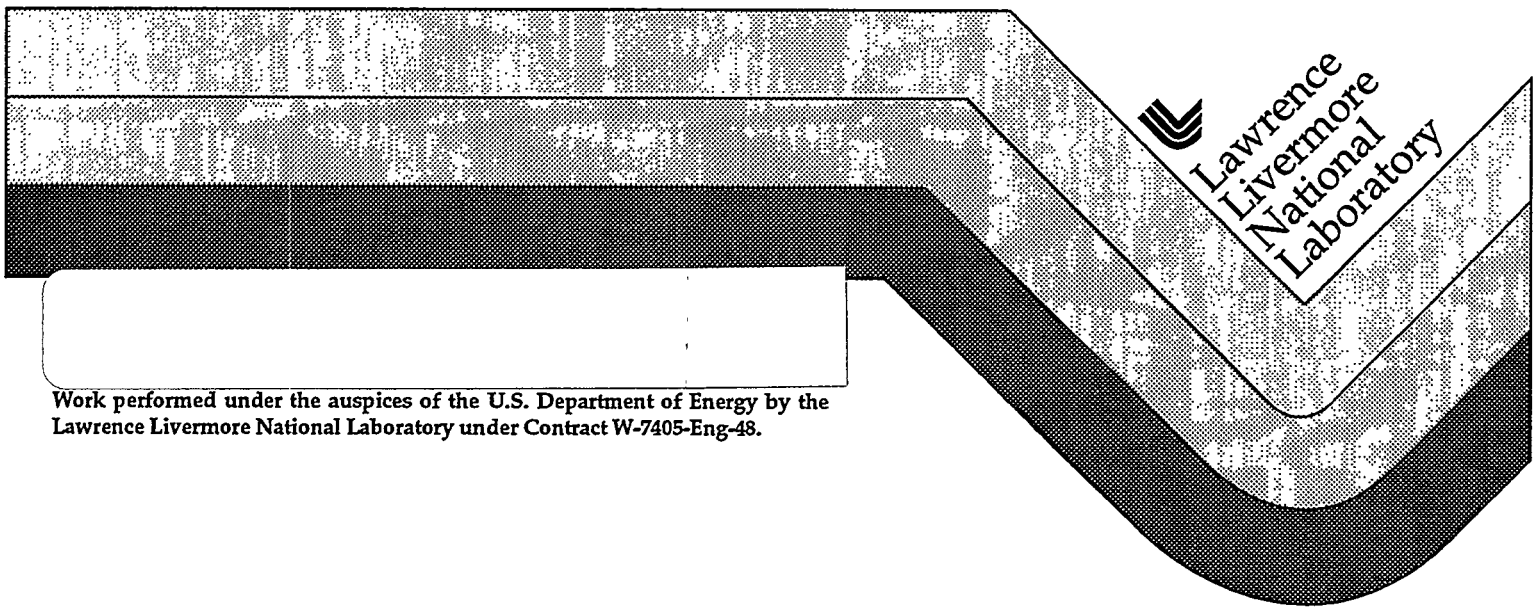

Work performed under the auspices of the U.S. Department of Energy by the Lawrence Livermore National Laboratory under Contract W-7405-Eng-48.

DISCLAIMER

WEXFORD Instrumentation Summary

Instrumentation	Fielded on this Event	Data Return	Present in this Report
Plug Emplacement	yes	yes	yes
Radiation	yes	yes	yes
Pressure			
Stemming	yes	yes	yes
Challenge	yes	yes	yes
Cavity	no	-	-
Atmospheric	no	-	-
Motion			
Free Field	no	-	-
Surface	yes	yes	yes
Plug	yes	yes	yes
Stemming	yes	yes	yes
Surface Casing	yes	yes	yes
Emplacement Pipe	yes	yes	yes
Hydroyield [a]	yes	yes	no
Collapse [b]	yes	yes	yes
Stress	yes	yes	yes
Strain [c]	yes	yes	yes
Other Measurements [d]	yes	yes	yes

(a) CORTEX or SLIFER in emplacement hole.
(b) EXCOR or CLIPER in emplacement hole.
(c) Emplacement pipe.
(d) Relative displacement between top plug and surface casing.

Event Personnel

Containment Physics	
B. Hudson	LLNL
C. Olsen	LLNL
J. Kalinowski	EG&G/AVO
T. Stubbs	EG&G/AVO

Instrumentation	
C. Cordill	LLNL
T. Brown	EG&G/AVO
B. W. Bellow	EG&G/NVO
A. E. Moeller	EG&G/NVO

Contents

1. Event Description

1.1 Site

The WEXFORD event was detonated in hole U2cr of the Nevada Test Site as indicated in Figure 1.1. A plan view map of the local region of hole U2cr showing the surface projections of the faults and the local drill holes is given in figure 1.2[1]. The device had a depth-of-burial of 314 m in the Tunnel Beds tuff of Area 2, about 120 m above the standing water level (SWL), as shown in Figure 1.3[1]. Stemming of the 2.44 m diameter emplacement hole followed the plan shown in Figure 1.4. A log of the stemming operations was maintained by Holmes & Narver[2].

Detonation time was 07:45 PDT on August 30, 1984 and about 26 minutes later the chimney collapsed to the surface leaving a small, off-center crater which grew, over several days, until it took on a "cookie cutter" form encompassing the emplacement hole and having a mean diameter of about 35 m. An interior, highly asymmetric crater had a mean diameter of about 12 m.

No functioning monitors detected radiation arrivals in the emplacement hole above a depth of 130 m and the WEXFORD containment was considered successful.

1.2 Instrumentation

Figure 1.5 is a schematic layout of the instrumentation designed to monitor the emplacement procedures and stemming performance of the WEXFORD event.

Three of the six stemming plugs (the first, fourth and fifth) were composed of coarse gypsum aggregate in a gypsum cement slurry. Each of these three gypsum-filled-aggregate (GFA) plugs was monitored during emplacement with arrays of conductivity probes and thermistors. Two of the remaining plugs were soft, coal tar aggregate (CT/A) gas seal membranes having a thickness of about 1.5 m sandwiched between layers of fines material. A layer of CT/A was poured on the top of each of the top two GFA plugs. An additional 4.2 m thick plug composed of two-part epoxy (TPE) was poured around the bottom of the surface casing. This plug was also topped with a layer of CT/A.

Pressure and radiation was monitored in the coarse stemming 4.7 m beneath the bottom surfaces of each of the top three solid plugs. Similar stations were fielded around the deepest CT/A plug (plug 2): 3.3 m above its top surface, and 4.3 and 6.1 m below its bottom surface. WEXFORD was the third event on which a multiplex system for transmitting the data from down-hole stations to the recording trailer was tested and two of the stations below the CT/A plug were included in this test. A duplicate pressure and radiation station was fielded 4.3 m below the plug as a control for one of the members of the multiplexed pair.

Pressure and radiation challenging the bottom GFA plug was measured through gas sample hoses penetrating the plug. The stations containing the transducers were mounted in the coarse stemming about 32 m above the top surface of the plug and the hoses extended through the plug to about 1 m above the device diagnostics canister. One of the hoses was terminated on its bottom with a fiber glass tube and the other with a wire rope screen as different methods for communicating with the challenge gas environment.

Vertical motion was monitored in plugs 4, and 5, on the surface casing, on the top of the emplacement pipe, at 0.61 m depth in the ground surface (15.24 m from SGZ), and in the recording trailer. Relative displacement between the surface casing and the top plug was monitored by an array of proximity switches located in the plug at the bottom of the surface casing. A geophone and a sensitive accelerometer were placed in the ground surface near the recording trailer.

Bi-axial stress and strain of the bottom GFA plug was monitored at four stations as part of a continuing transducer development program..

Data from each of the above transducers were transmitted to the recording trailer by an analog system and recorded on magnetic tape.

One CLIPER/CORRTEX sensor was emplaced, as indicated in figure 1.5, to measure the hydrodynamic yield of the device and to monitor cavity collapse and chimney formation. Results of the yield measurements are reported elsewhere[3].

A history of the fielding operations of the instrumentation, including the emplacement pipe strain measurements, is outlined in reference 4. Details of the instrumentation are given in reference 5.

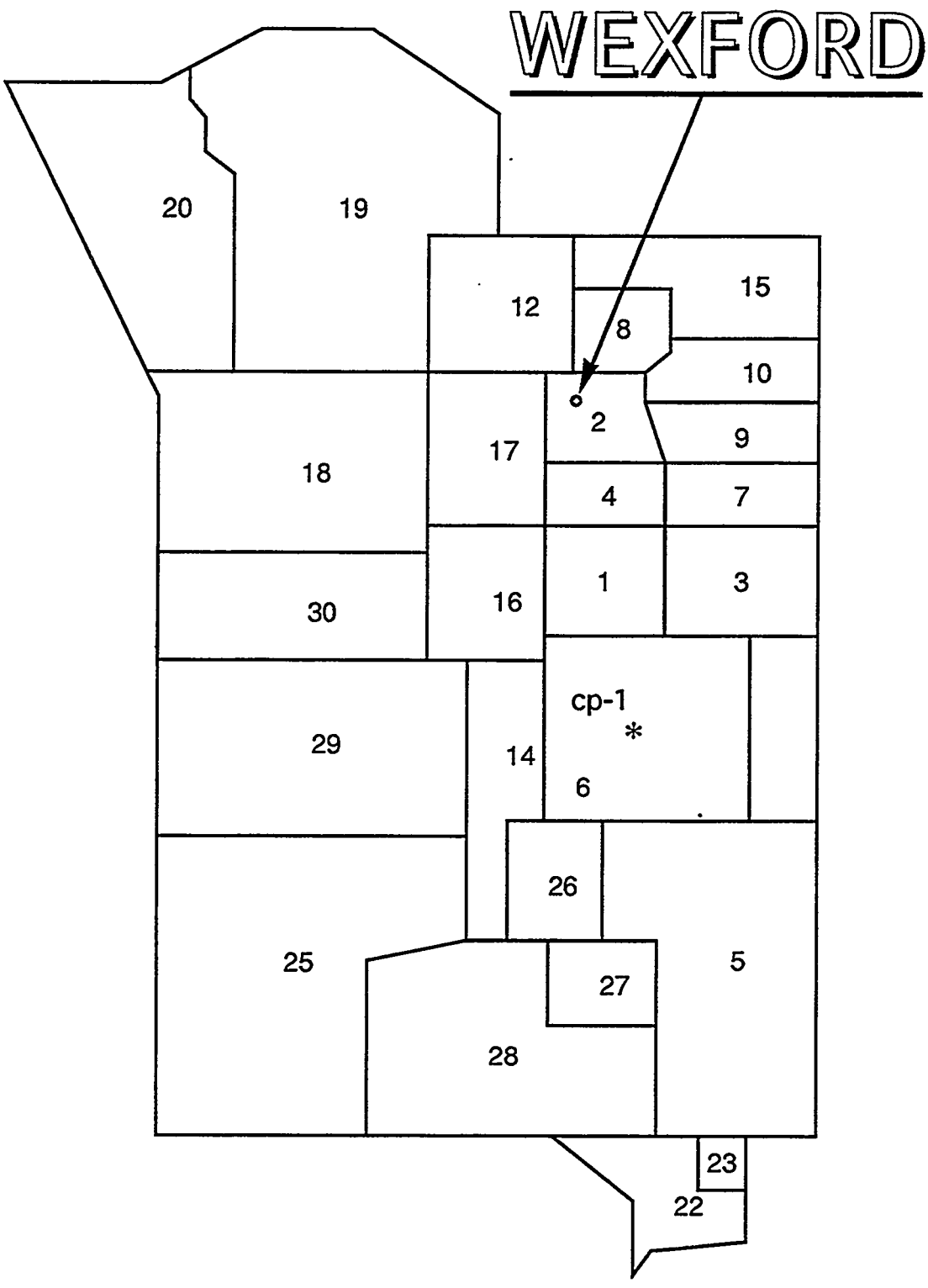

Figure 1.1 Map of the Nevada Test Site indicating the location of hole U2cr.

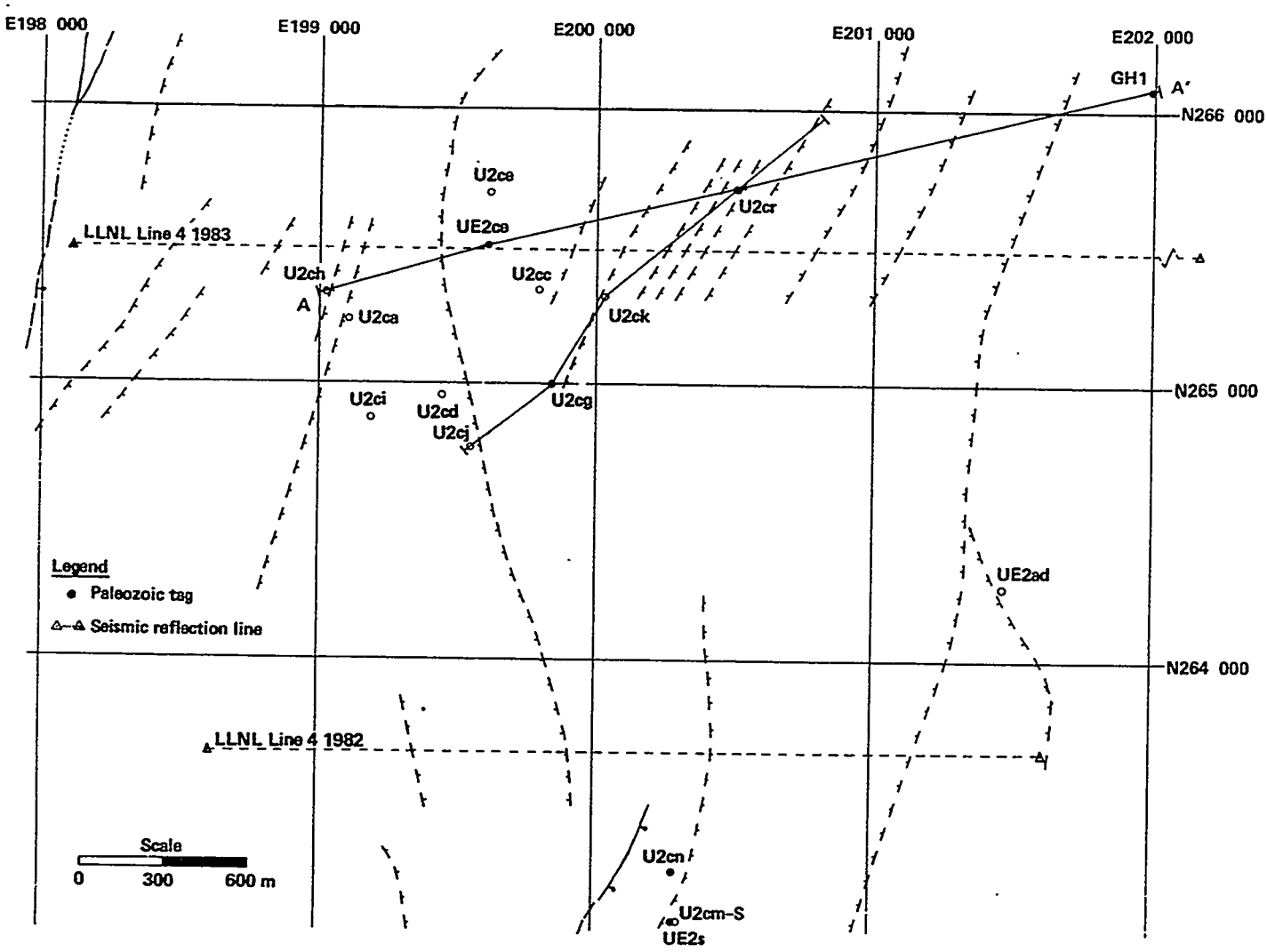

Figure 1.2 Plan view map of the U2cr site.

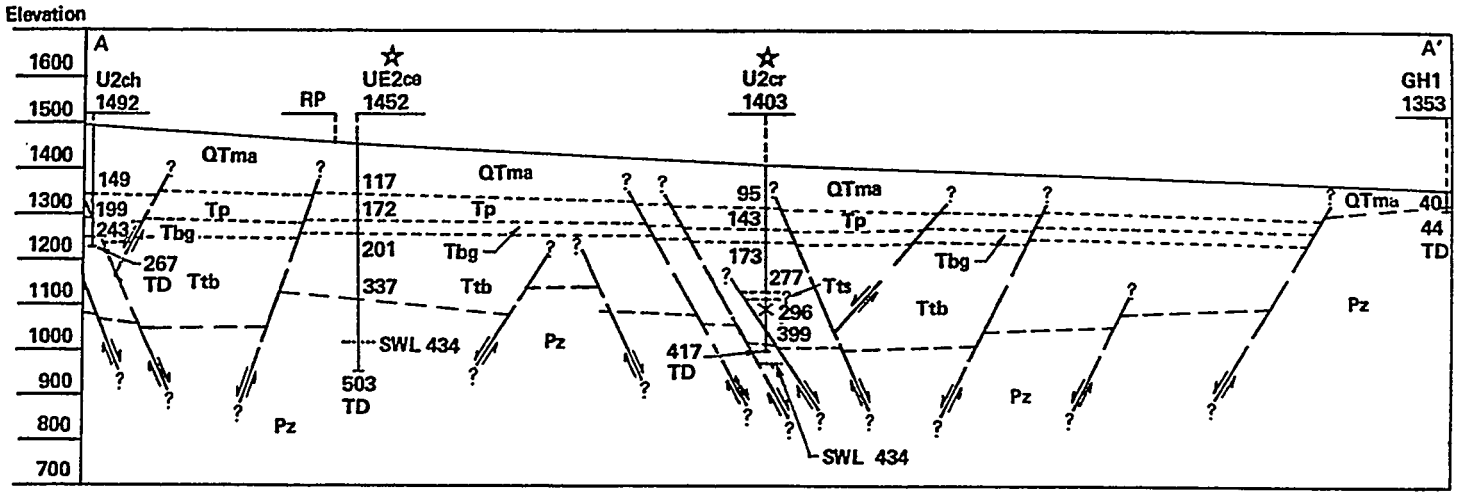

Scale

0 300 600 m

Geologic Cross Section A-A'
U2cr

GAP 2-21-84

Legend

QTma	Mixed Alluvium
Tp	Paintbrush Tuff
Tbg	Grouse Canyon Airfall
Ttb	Tunnel Beds
Tts	Tub Spring Tuff
Pz	Paleozoic sedimentary rocks
?–?	Inferred fault based on seismic and/or gravity data
☆	Bend in section
SWL	Static water level
RP	Seismic reflection reference point

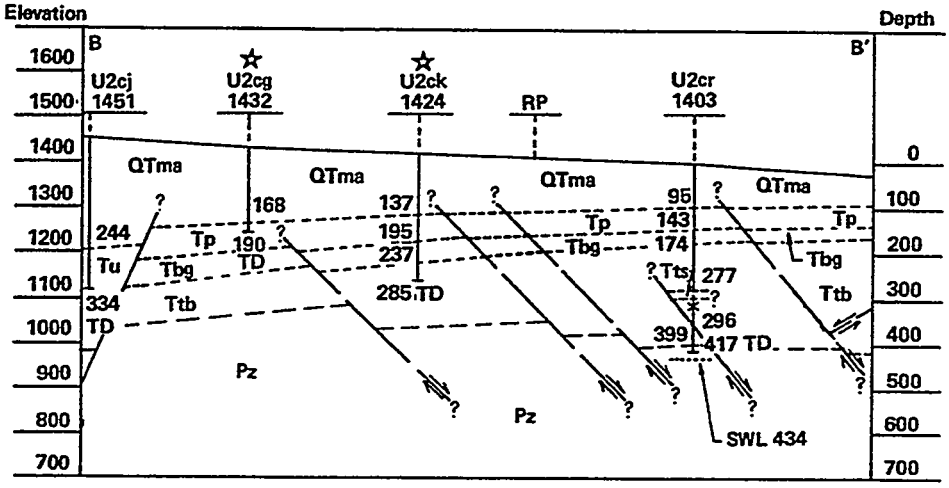

Figure 1.3 Geologic cross sections through hole U2cr.

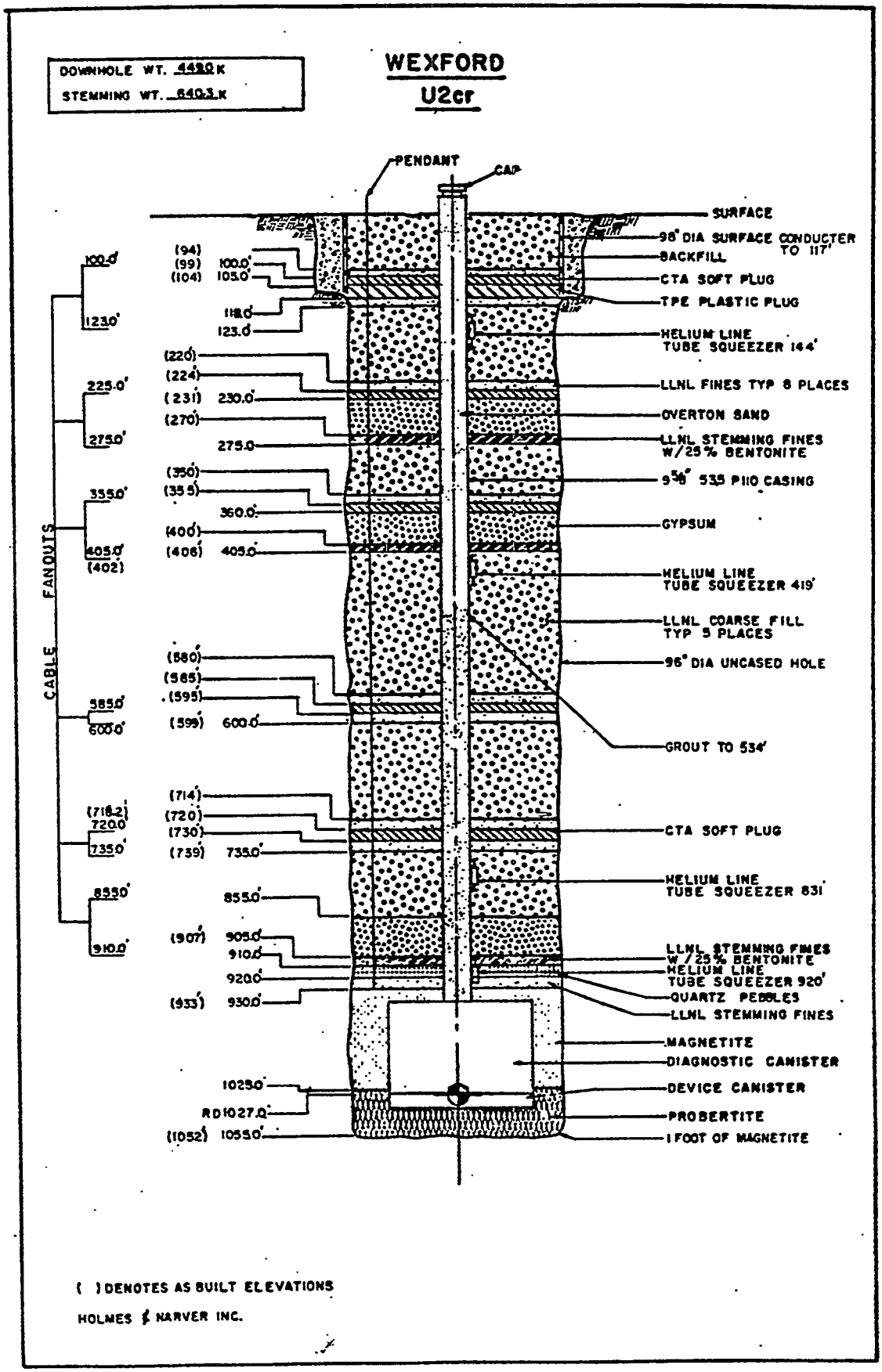

Figure 1.4 As-built stemming plan for the event WEXFORD in Hole U2cr.

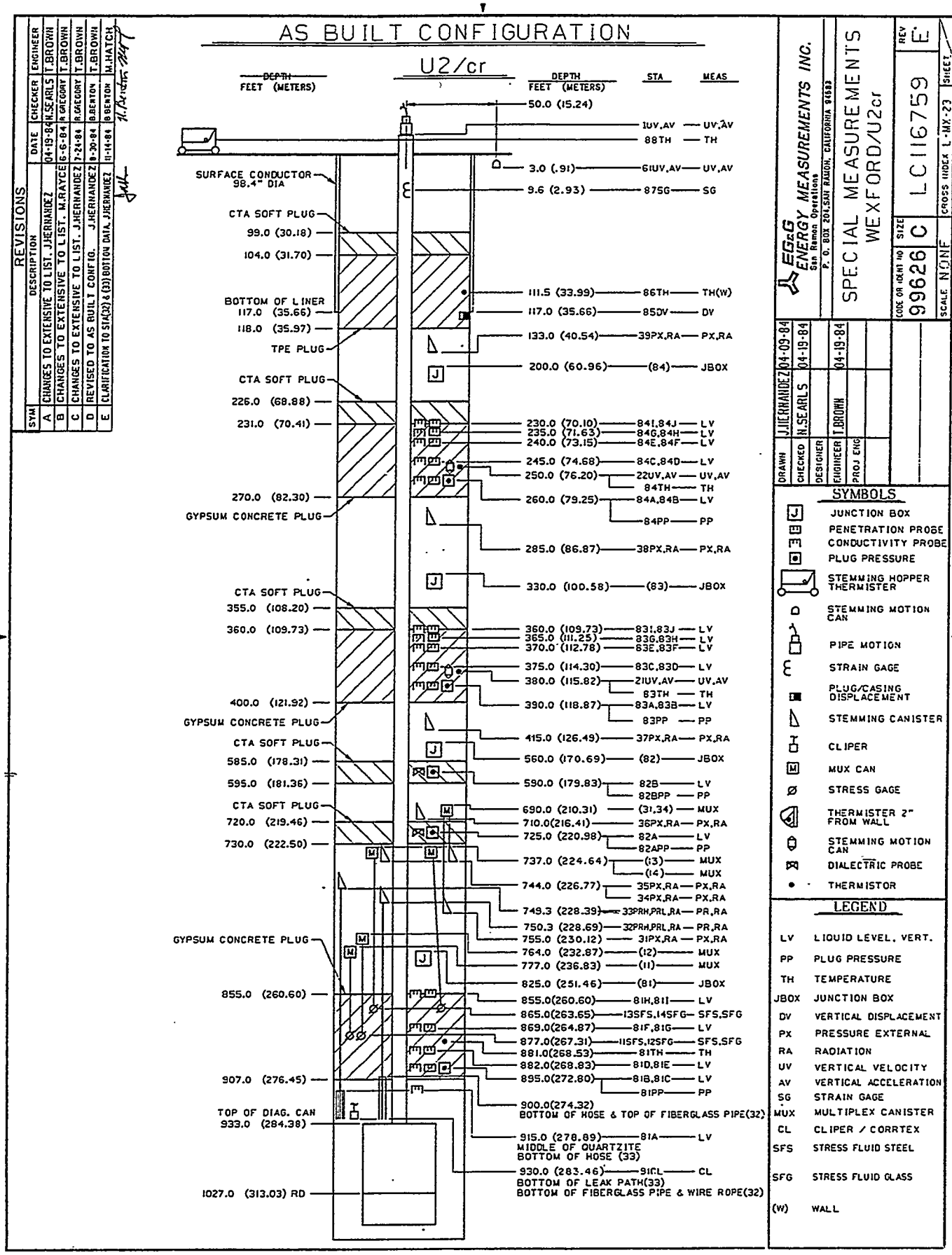

Figure 1.5 As-built containment instrumentation plan for the WEXFORD event.

2. Emplacement

2.1 Pipe strain

Figure 2.1 is the strain history measured on the emplacement pipe during stemming of the WEXFORD experiment. The emplacement pipe was instrumented with a strain gage station on the final pipe section just below the load collar (Station 87). These data were also reported in reference (6).

2.2 Plug levels and temperature

The emplacement of each of the three gypsum concrete plugs was monitored with an array of dielectric and conductivity probes and thermistors. The locations of the probes are tabulated in figure 1.5. The upper and lower boundary positions of the plugs were determined by tag lines. Figure 2.2 contains plots of the arrival times of the GFA slurry as a function of depth (as determined from the conductivity probes and tag lines). Temperature sensors were fielded in each concrete plug, however, the data from these are not available. All plugs were emplaced as planned.

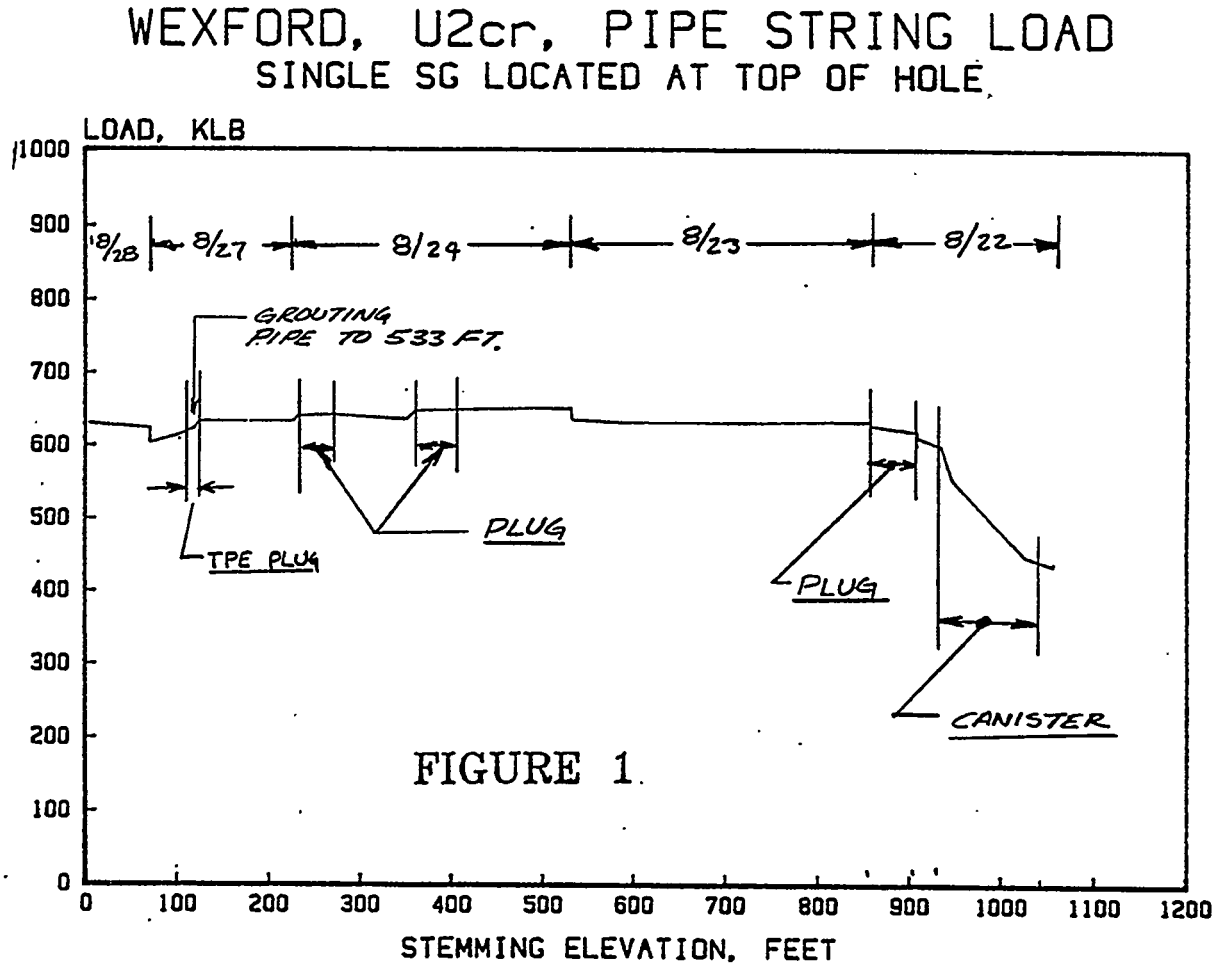

FIGURE 1.

Figure 2.1 Strain measurements during the stemming at stations 87 (near the top of the pipe). Data are taken directly from reference 6.

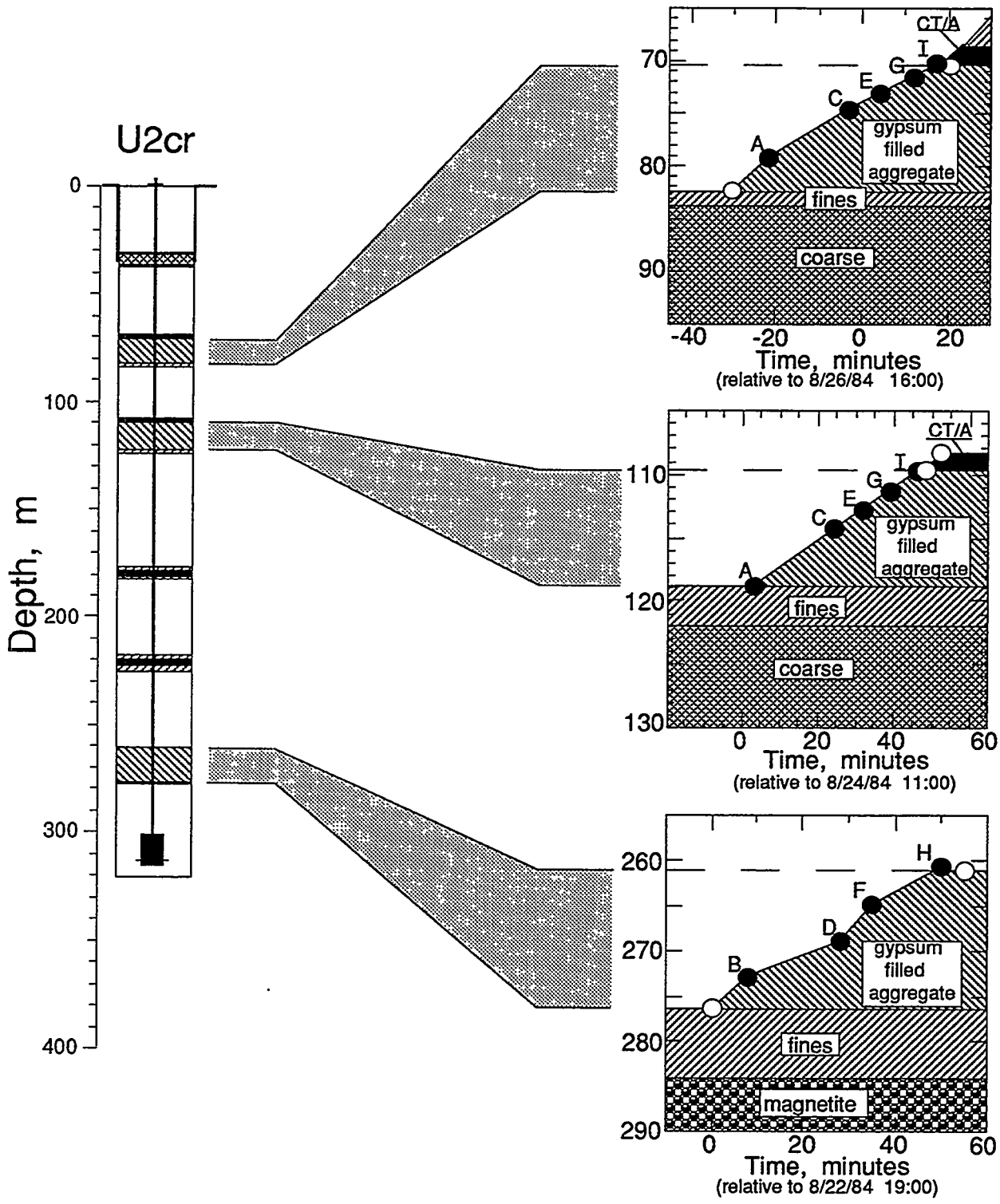

Figure 2.2. Emplacement diagnostics data for the GFA plugs. The upper and lower boundaries of the plugs were determined with a tag line. Solid symbols indicate the elevations of the probes and the open symbols are at the tag depths. A temperature sensor was located between probes "B" and "D" on plug 1 and between probes "A" and "C" on plugs 4 and 5.

3. Stemming Performance

3.1 Radiation and Pressure

As seen in figure 1.5, the coarse stemming around the deepest soft CTA plug and below the top three solid plugs was monitored for radiation and pressure. Also challenge pressure and associated radiation was measured below the deepest GFA plug. The signals were transmitted to the recording trailer in analog form and recorded on magnetic tape for later processing.

Pressure and radiation histories from a few seconds before detonation until about 200 s after loss of signal at cavity collapse (about 27 minutes later) are shown in figures 3.1–3.8. Figure 3.9 shows the pressure and radiation recorded at the station just below the top TPE plug from about 200 s before detonation to about 9000 seconds later (the full time of recording).

WEXFORD was the third experiment on which a down-hole multiplex (MUX) system (composed of stations 31 and 34) was installed to transmit containment data to the recording trailer. To serve as a control for verification of the data from the MUX, station 35 was fielded with the same instrumentation and at the same elevation as station 34 (just below the deepest soft CTA plug). The impedance to gas flow afforded by this soft plug was monitored by a radiation and pressure station immediately above it (station 36).

All pressure and radiation data are consistent with satisfactory containment.

3.1.1 Pressure

The pressure record obtained from station 31 (figure 3.1) is likely to be erroneous, in view of the data from the other stations. Causes of this are uncertain.

Stations 32 and 33 were connected to the coarse stemming below the deepest GFA plug through sections of gas sample hose (GSH) to monitor the pressure challenging that plug. The GSH of station 32 was extended from just inside the lower surface of the plug to a position about 1 m above the device canister by a fiber glass tube. The GSH associated with station 33 was extended by a wire rope screen from about 2 m below the plug to the same bottom elevation as the extension of station 32. Á priori, it was unknown which of the two would provide the better coupling to the challenge pressure environment, so both were employed. Data obtained from these two stations are shown in figures 3.2 and 3.3 and are compared in figure 3.10. For times greater than 500 s after detonation, the two records are identical. At earlier times, however, the data suggest that the wire rope screen affords a better coupling between the transducer and the challenge pressure gas. The slight pressure rise seen after 1300 s, prior to signal loss, is suggested to be due to a stretching of the GSH as a result of stemming fall.

Station 34 (just below the first soft plug) shows an explosion-induced pressure jump of about 3.5 psi with a late-time drop of abut 1 psi corresponding to the times of pressure increase seen in the GSH. Station 35, the sister station to 34, shows a similar initial pressure jump but its later wave form is noisy.

An explosion-induced pressure increase at zero time of about 1.5 psi is maintained at station 36 (figure 3.6) for the full period that the station remains active. This suggests that the soft plug can maintain a pressure differential of at least 2 psi. The late-time pressure changes (at times greater than 1300 s) evidenced at stations below the plug is not seen in station 36.

The pressure and radiation in the coarse stemming immediately below the TPE plug at the bottom of the surface casing was monitored by station 39. The explosion produced an early time pressure rise which reached its peak about 0.6 psi above ambient at 15 seconds after the detonation, decaying to ambient 100 seconds later. At collapse time, (1596 s) a pressure drop of about 3 psi was noted. The pressure returns to ambient in stages at about 1 hour. This behavior is characteristic of a stemming fall below the recording station.

3.1.2 Radiation

Figures 3.1–3.5 show at least two radiation arrivals in the data collected below the deepest soft CT/A plug. A first radiation front arrives within the first 50s, while a second, major pulse of radiation arrives between 100 and 200 s. A composite of the radiation histories displaying the first arrivals of radiation measured at the stations below the deepest soft CT/A plug is shown in figure 3.11. Excluded from this, for clarity, are the data of station 34 as they are identical with those from station 35 (see figures 3.4 and 3.5).

The wave forms of the radiation at times greater than about 250 s are the same for stations 31–35 (except for amplitude) suggesting that all stations have a common late-time source. A source of radiation at early times is suggested by comparing the wave form of the gas pressure measured in the gas sample hose of station 33 with that of the radiation measured in the stemming at station 31 (figure 3.13). The similarity is striking.

To see if the gas in the hose of station 33 can be a source seen by station 31 we make the following assumptions.

1. The GSH of station 33 is open to the challenge gasses.
2. The challenge gas is well mixed with radioactive material.
3. There are no leaks in the GSH.
4. The GSH maintains its dimensions during pressurization.

Let L_0 be the initial length of the gas column in the GSH = 50.5 m
p_0 be the initial pressure in the GSH = 12.5 psia
p_f be the final measured pressure in the GSH = 595 psia

Then the full length of the compressed air (non-radioactive) column, L, is given by:

$$L = L_0 * \left(\frac{p_0}{p_f}\right) = 1.05m$$ Isothermal compression

or

$$L = L_0 * \left(\frac{p_0}{p_f}\right)^{\frac{1}{1.4}} = 3.19m$$ Adiabatic compression.

Figure 3.13 is a sketch showing the relative vertical positions of stations 31–36. The level of the interface between the radioactive and non-radioactive gas in the GSH of station 33 is indicated, depending on whether the compression was adiabatic or isothermal. This shows that, if the compression was isothermal, the radiation front would be above the level of station 31 and suggests that the GSH and wire rope screen combination yielded good challenge pressure communication to the transducer of station 33. Assumption 4, above, is the least likely to be met and expansion of the GSH, under pressure, will lower these elevations.

The close comparison of the radiation histories of stations 34 and 35 (figures 3.4 and 3.5) validate the use of down-hole multiplex electronics for data transmission.

The recorded ambient radiation level at station 36 was greater than 40,000 R/Hr and was thus considered to be false and is not reported. There is, therefore, no radiation information on the gas impedance of CT/A plug 2.

No further radiation arrivals were detected in the emplacement hole before collapse. Station 39 (figure 3.9) shows a low-level offset in the radiation history at about 6200 s. The character of this offset suggests that it may have been caused by recording system malfunction, although the presence of radiation can not be ruled out.

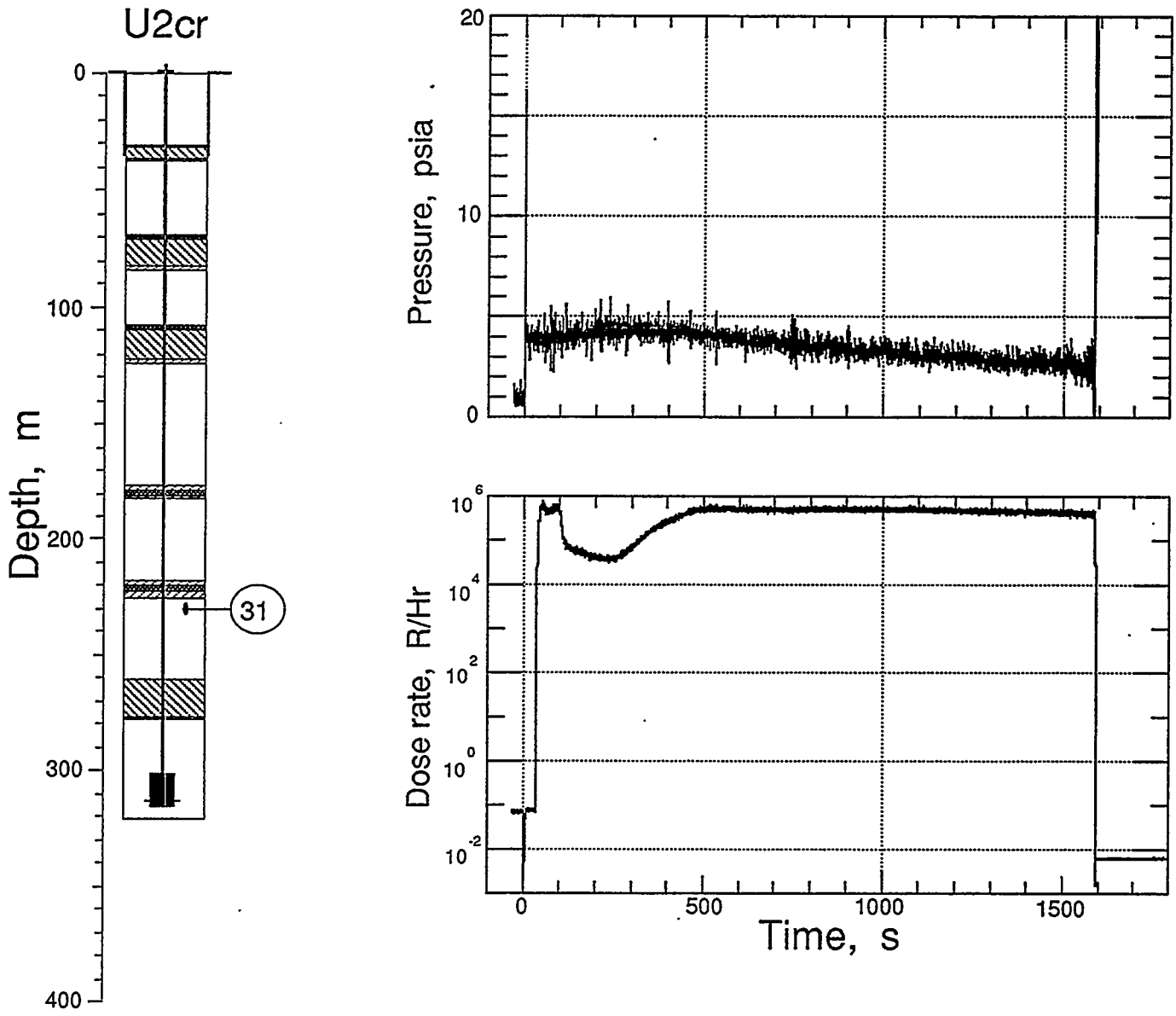

Figure 3.1 Pressure and radiation measured in the coarse stemming between the deepest GFA plug 1 and the gas seal plug 2 (Station 31 at 230.1 m depth). First radiation arrival was at 35 s. Signals were lost at collapse time (1589 s). This station was multiplexed with station 34.

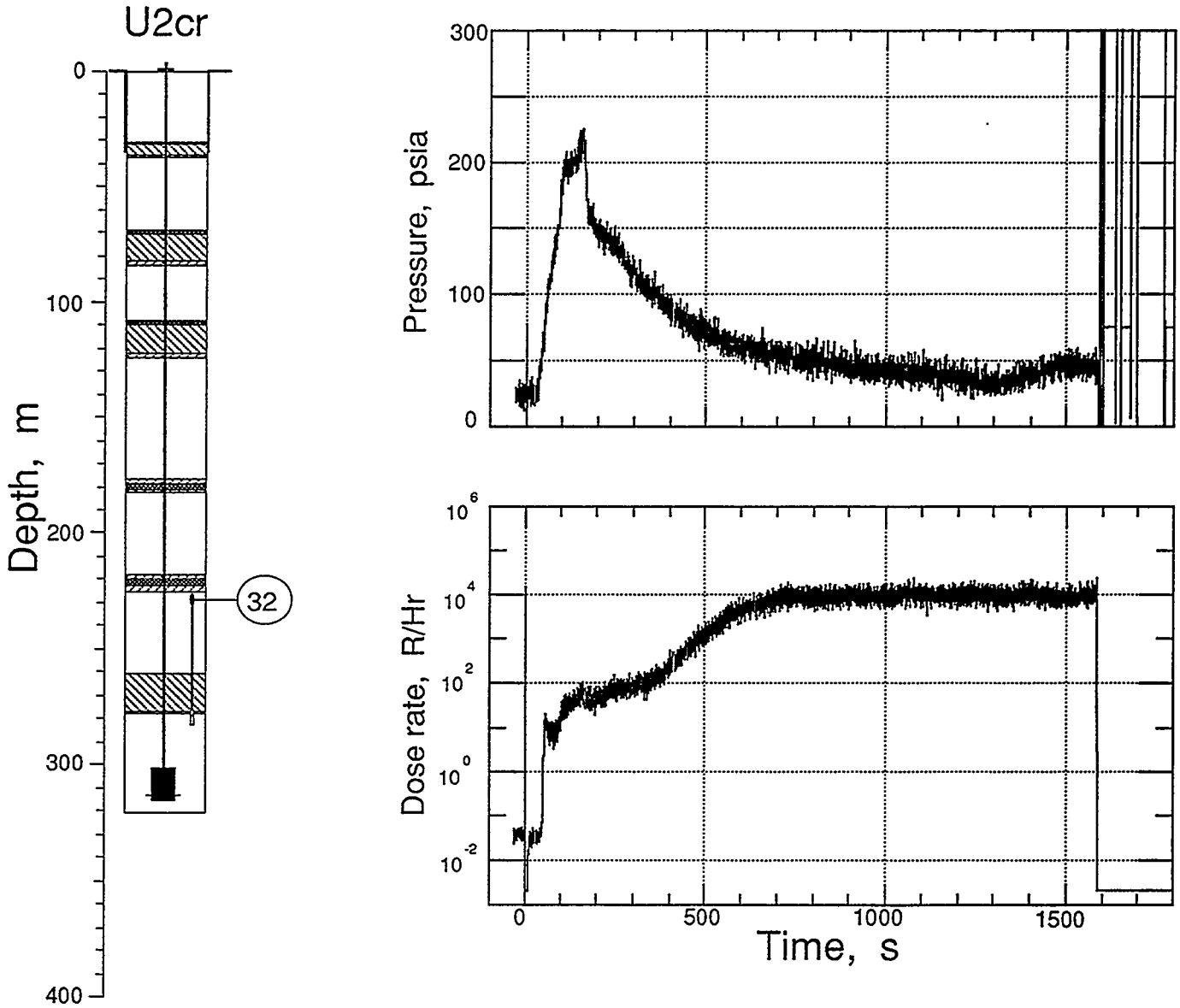

Figure 3.2 Pressure challenging the deepest plug (station 32) at a depth of 228.7 m. Gas pressure was sensed through a section of wire rope (gas sample hose) extended by 9.14 m by a fiber glass pipe to a depth of 283.46 m. First radiation arrival was at 41 s. Signals were lost at collapse time (1589 s).

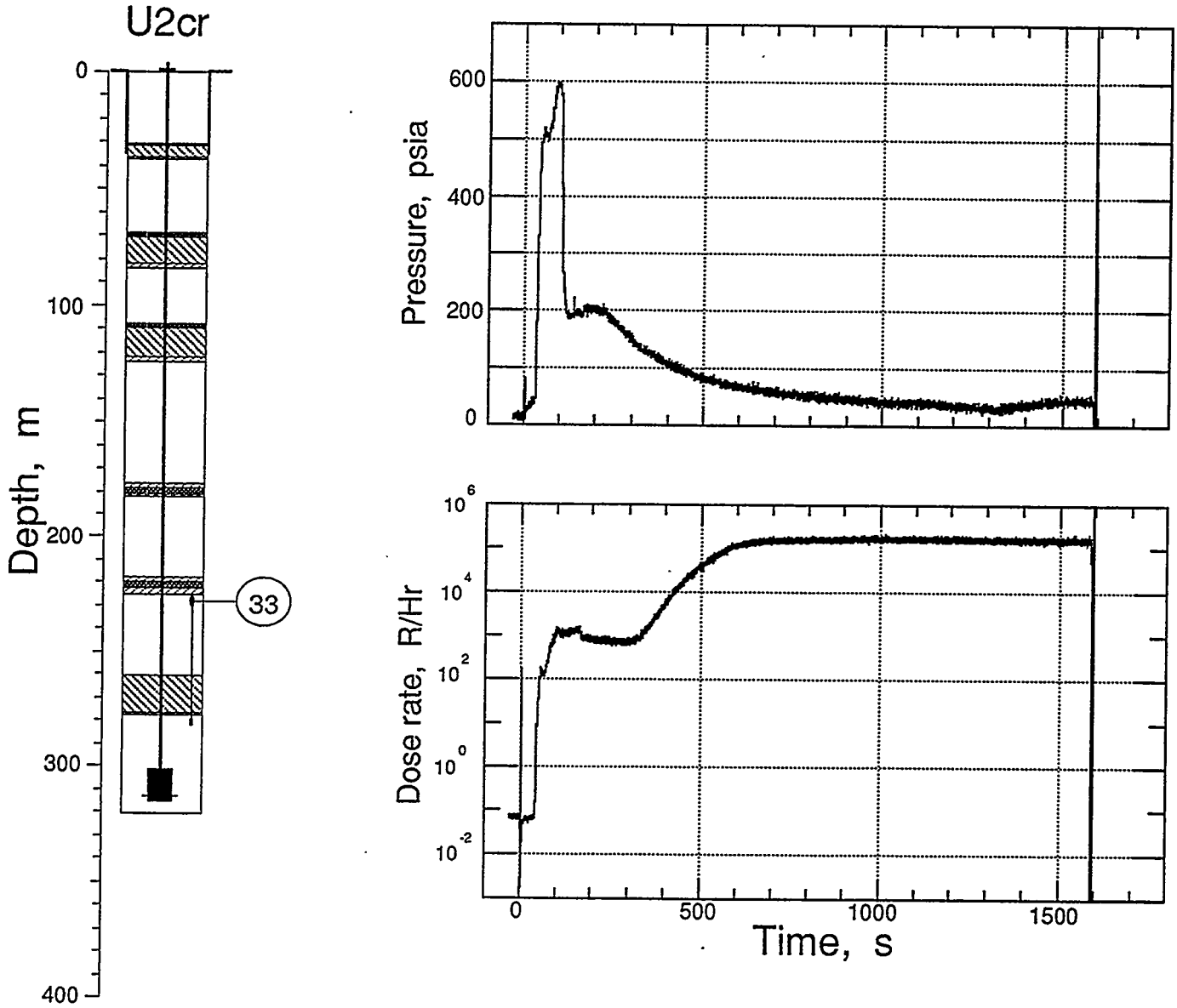

Figure 3.3 Pressure and radiation challenging the deepest plug (station 33) at a depth of 228.4 m. Gas pressure was sensed through a section of wire rope (gas sample hose) extended by 4.57 m by a braided wire rope screen to a depth of 283.46 m. First radiation arrival was at 39 s. Signals were lost at collapse time (1589 s).

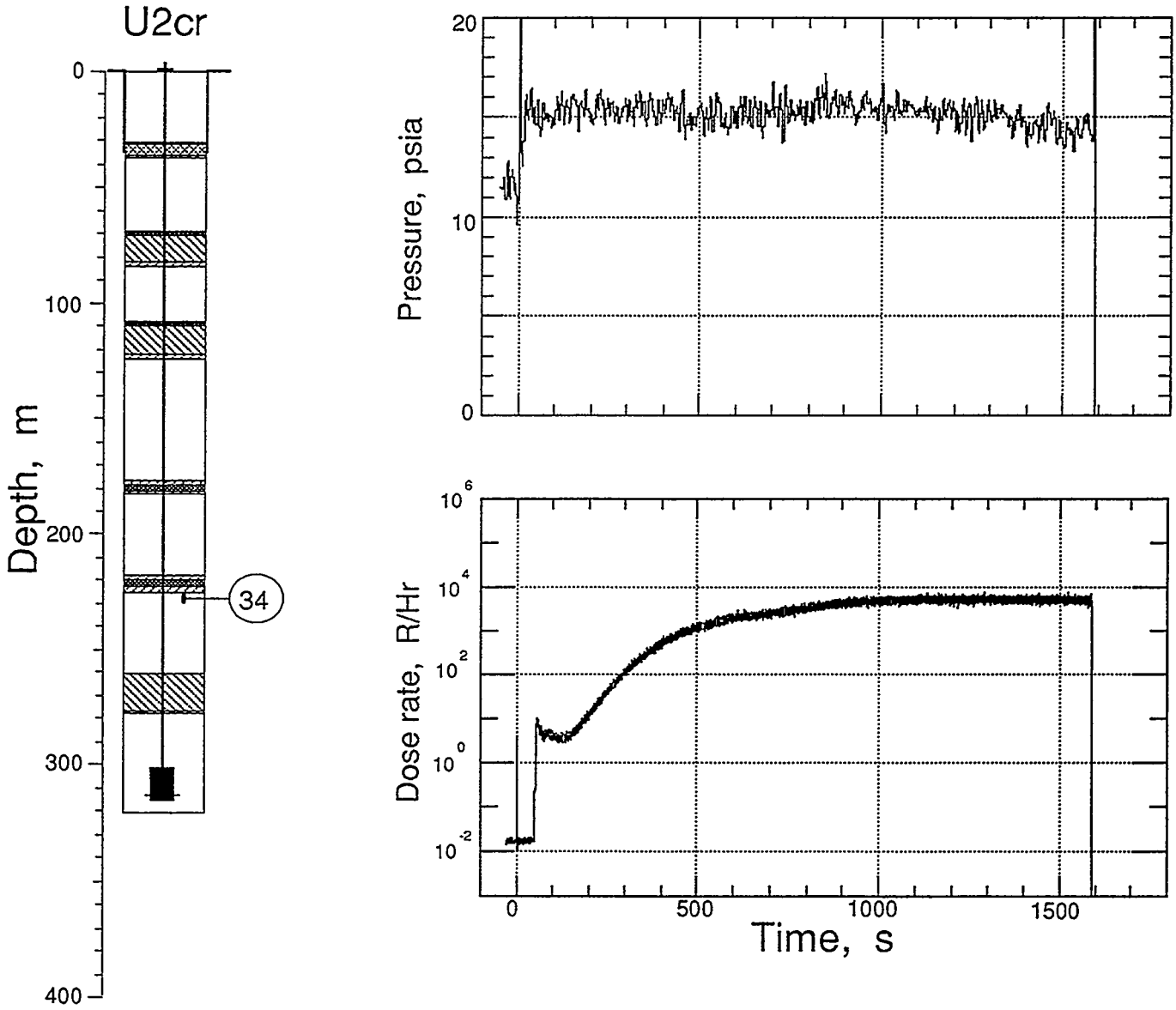

Figure 3.4 Pressure and radiation measured in the coarse stemming below gas seal CT/A plug 2 at a depth of 226.8 m (station 34). First radiation arrival was at 50 s. Signals were lost at collapse time (1589 s). This station was multiplexed with station 31.

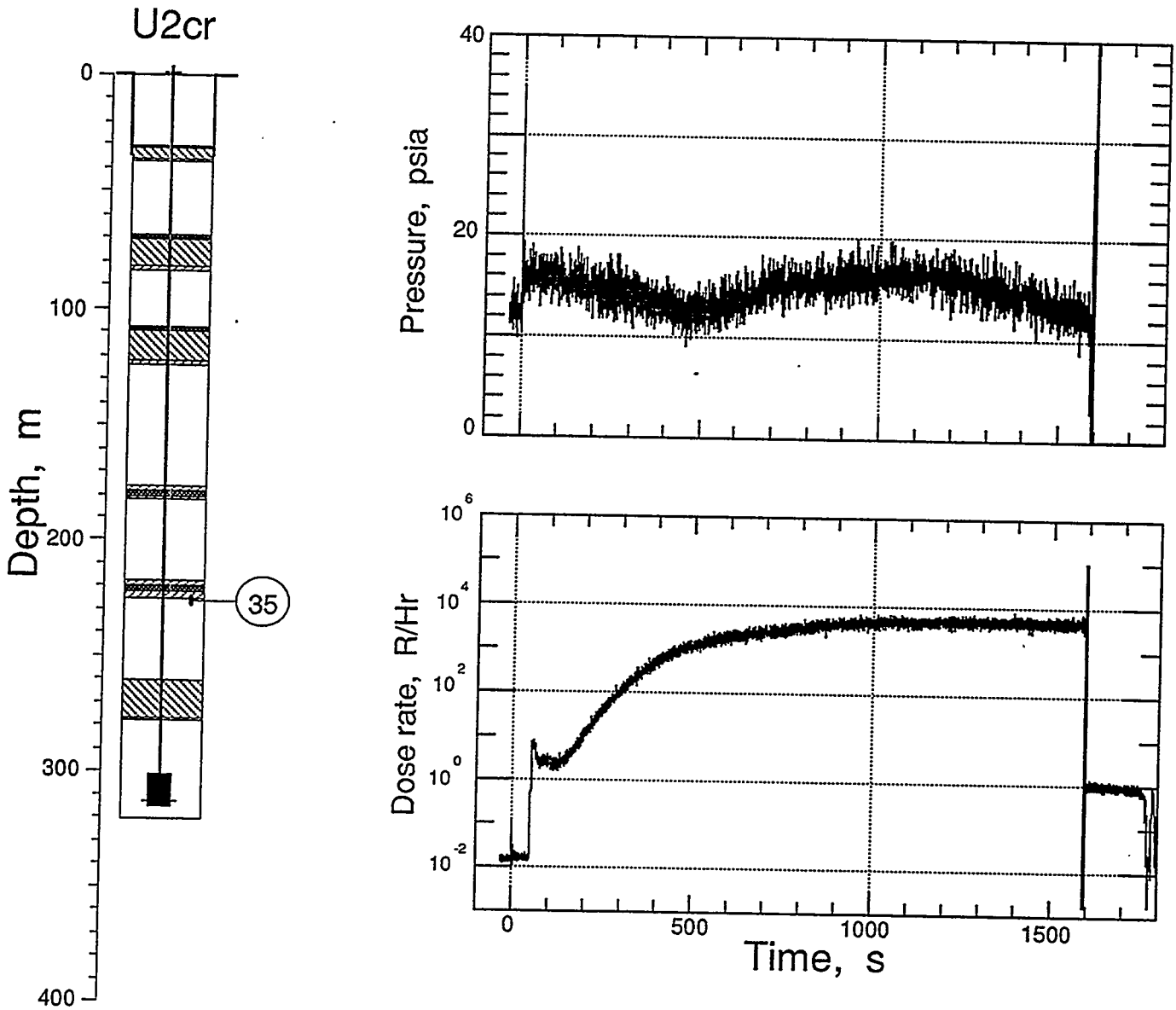

Figure 3.5 Pressure and radiation measured in the coarse stemming below gas seal CT/A plug 2 at a depth of 226.8 m (station 35). First radiation arrival was at 50 s. Signals were lost at collapse time (1589s).

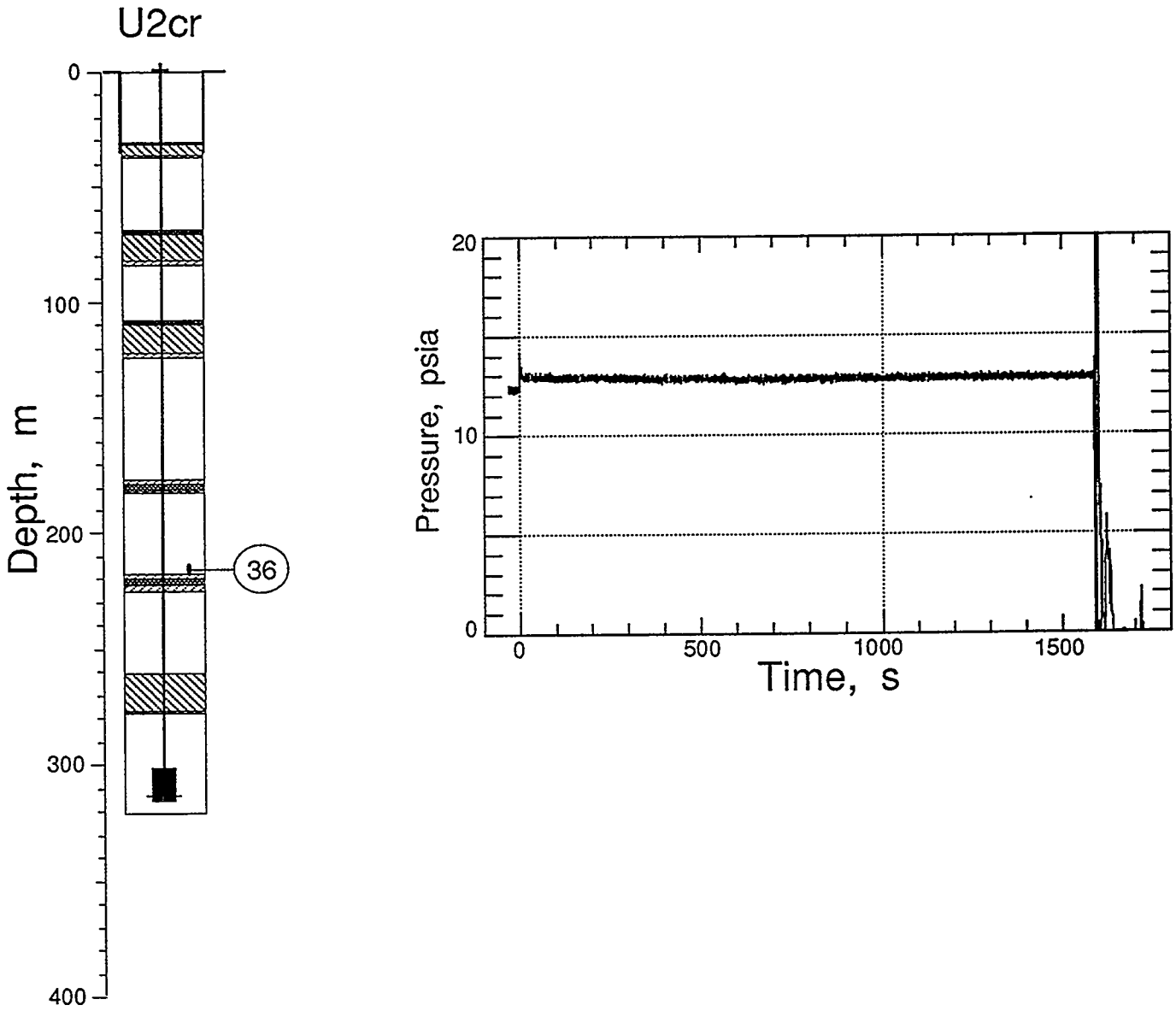

Figure 3.6 Pressure measured in the coarse stemming above gas seal CT/A plug 2 at a depth of 216.4 m (station 36). Signals were lost at collapse time (1593 s). Radiation levels pre-shot registered greater than 40,000 R/Hr and were thus considered false and not reported.

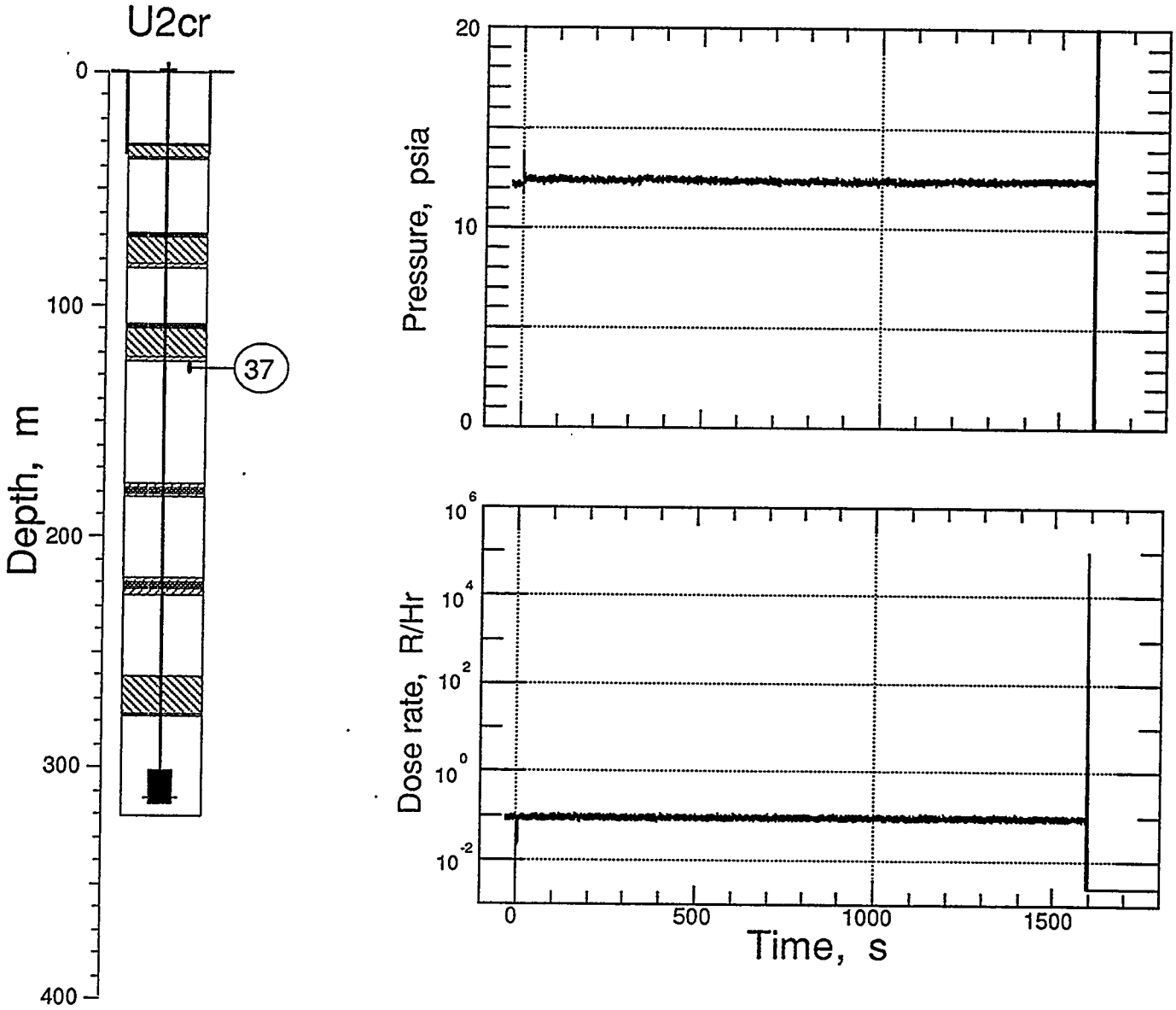

Figure 3.7 Pressure and radiation measured in the coarse stemming below GFA plug 4 at a depth of 126.5 m (station 37). Signal was lost at collapse time (1594 s).

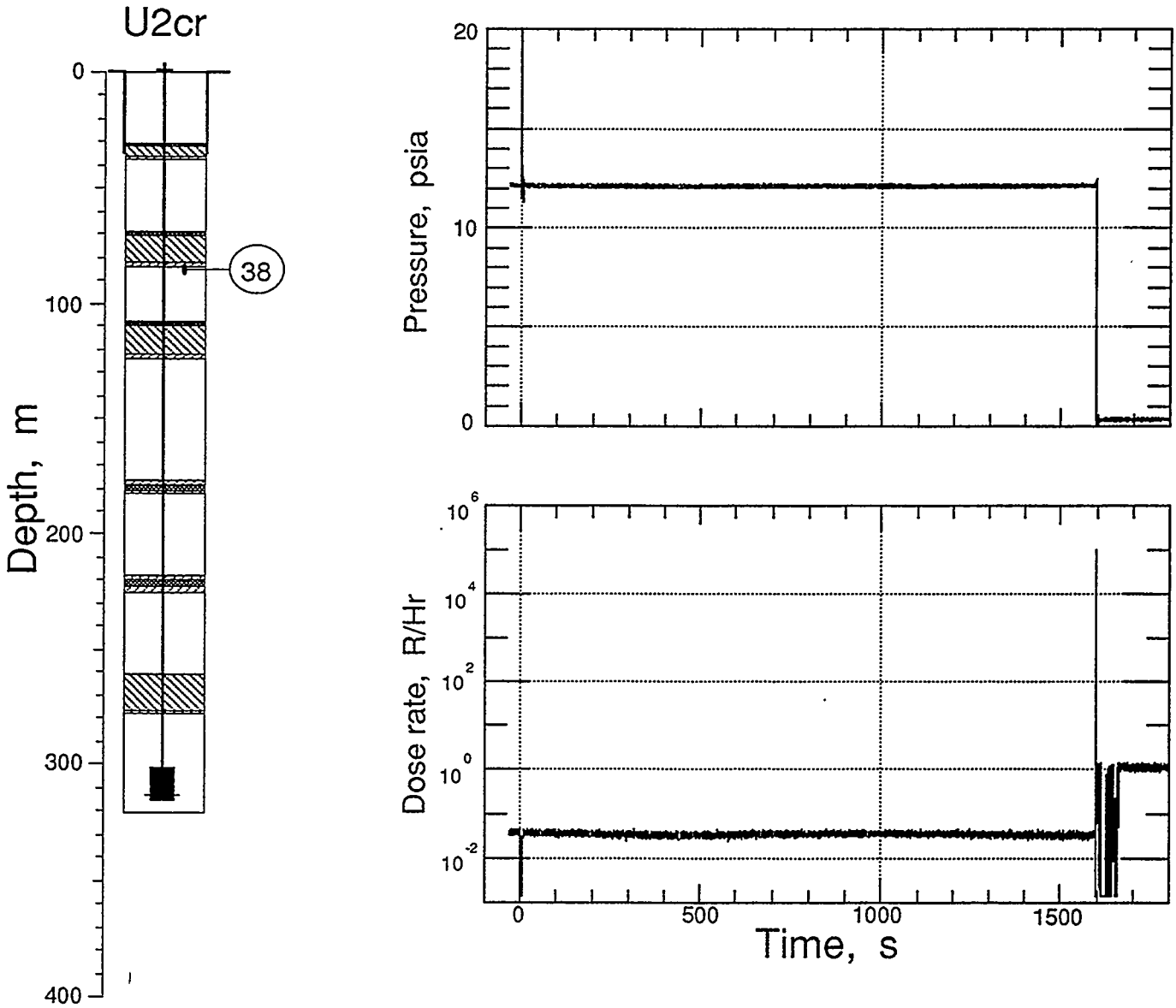

Figure 3.8 Pressure and radiation measured in the coarse stemming below GFA plug 5 at a depth of 86.9 m (station 38). Signals were lost at collapse time (1596 s).

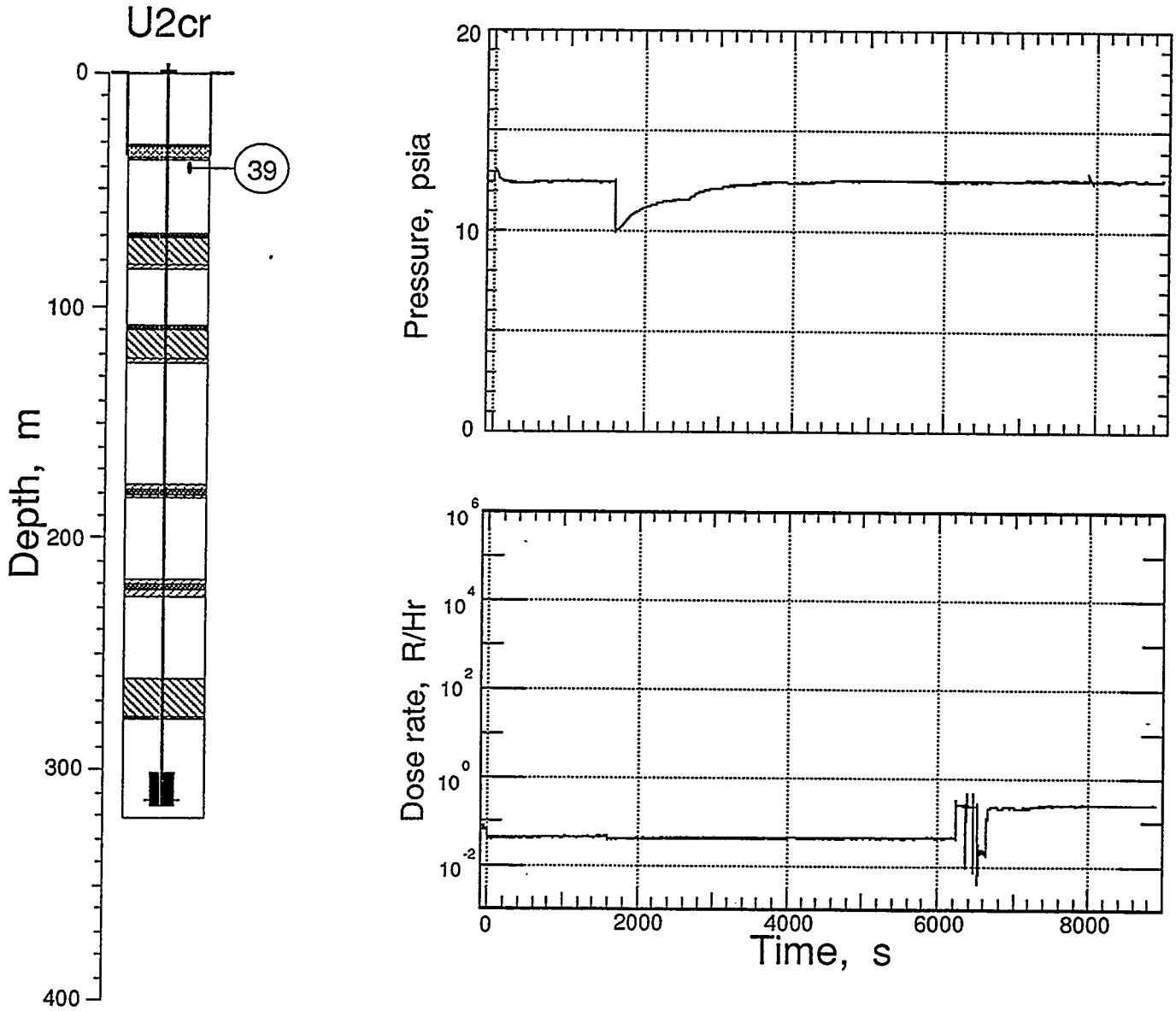

Figure 3.9 Pressure and radiation measured in the coarse stemming below the top TPE plug at a depth of 40.5 m (station 39). Signals were never lost during the entire period of recording, although the radiation channel seems to have been offset at about 6200 s.

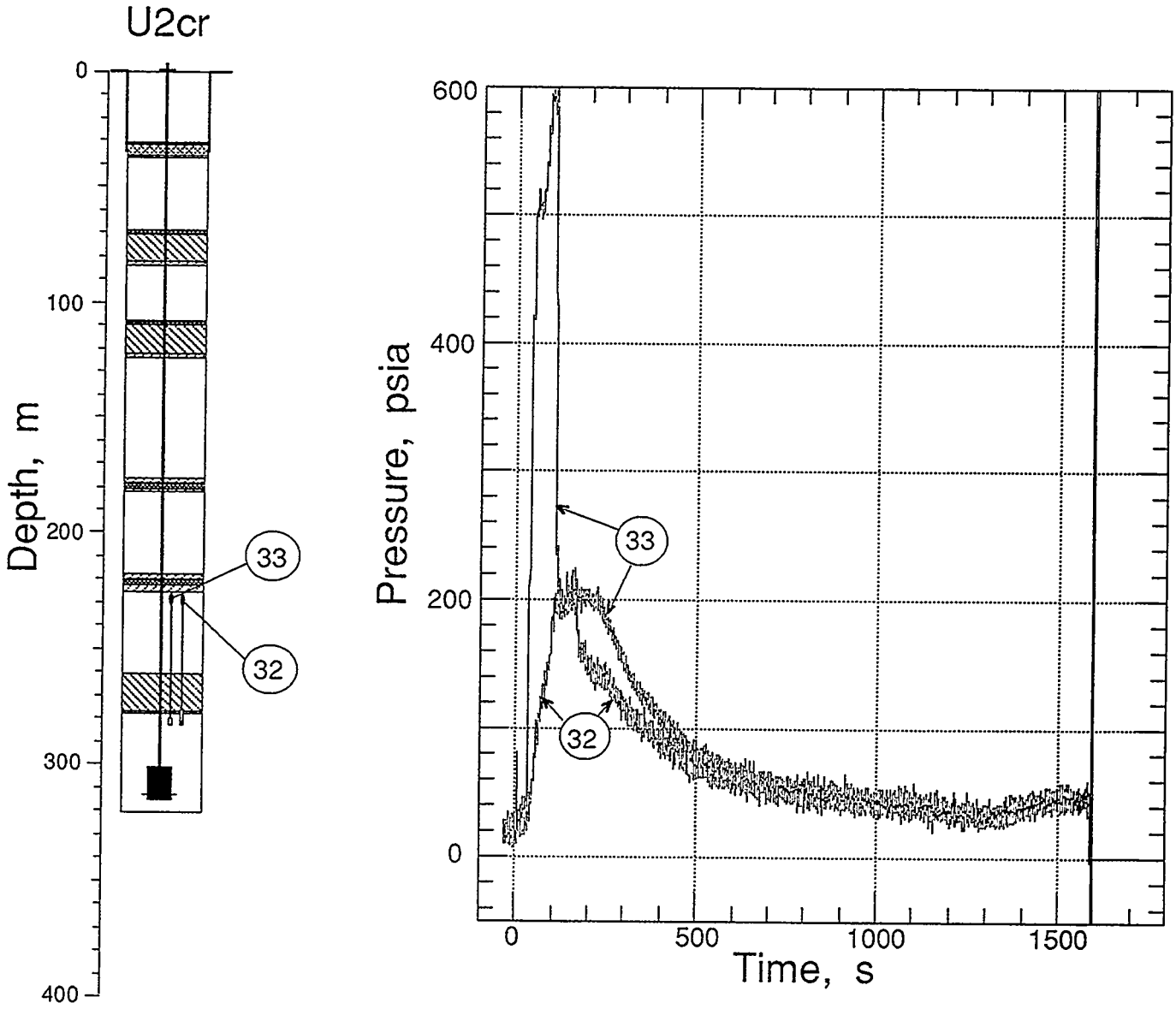

Figure 3.10 Comparison of the challenge pressures measured at stations 32 and 33. Station 32 extended the 45.63 m long GSH by 9.14 m through a fiber glass tube to a depth of 283.46 m. Station 33 extended the 50.5 m long GSH by 4.57 m through a wire rope screen to a depth of 283.46 m.

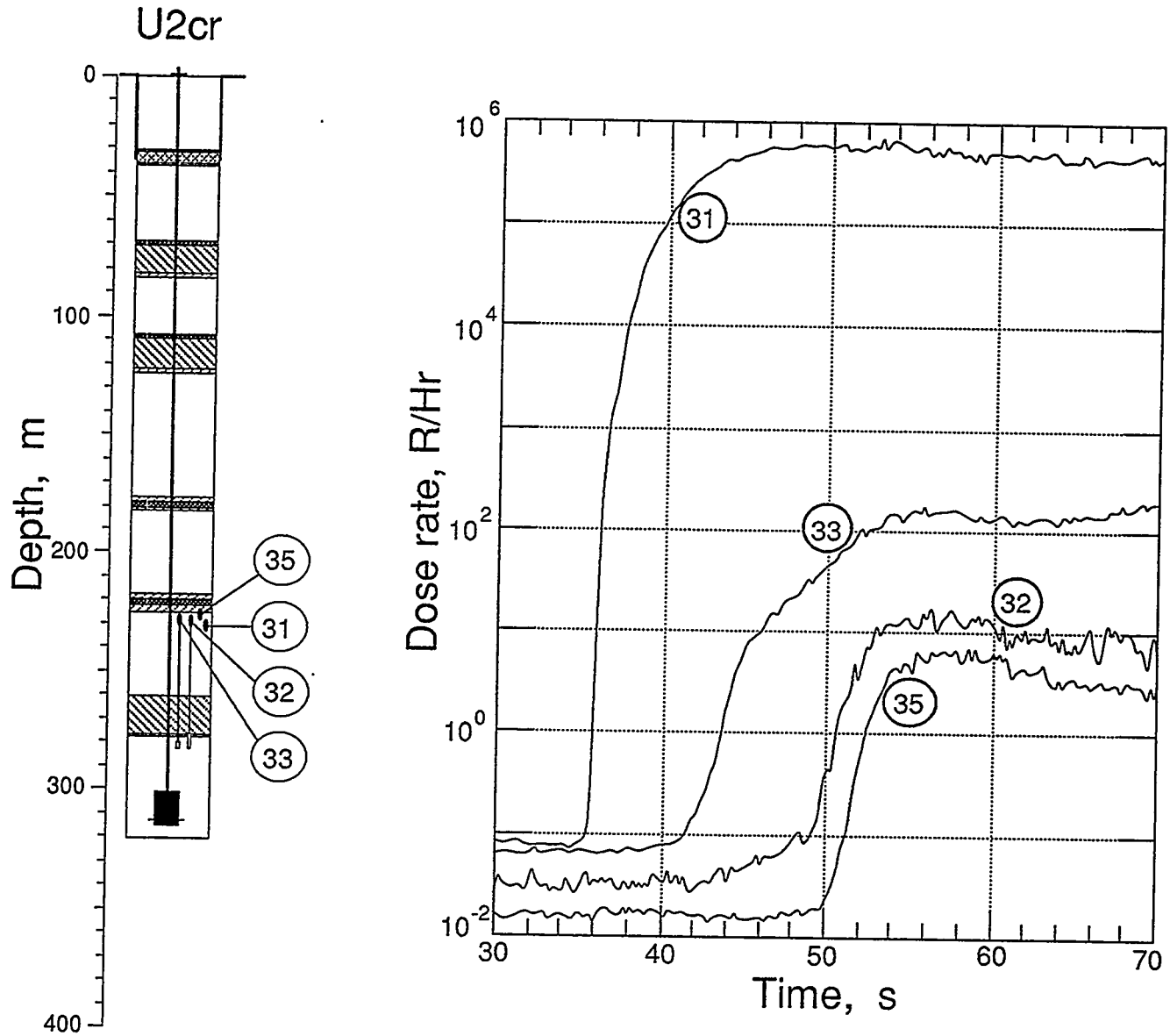

Figure 3.11 Composite of the radiation wave forms from stations below the deepest CT/A plug.

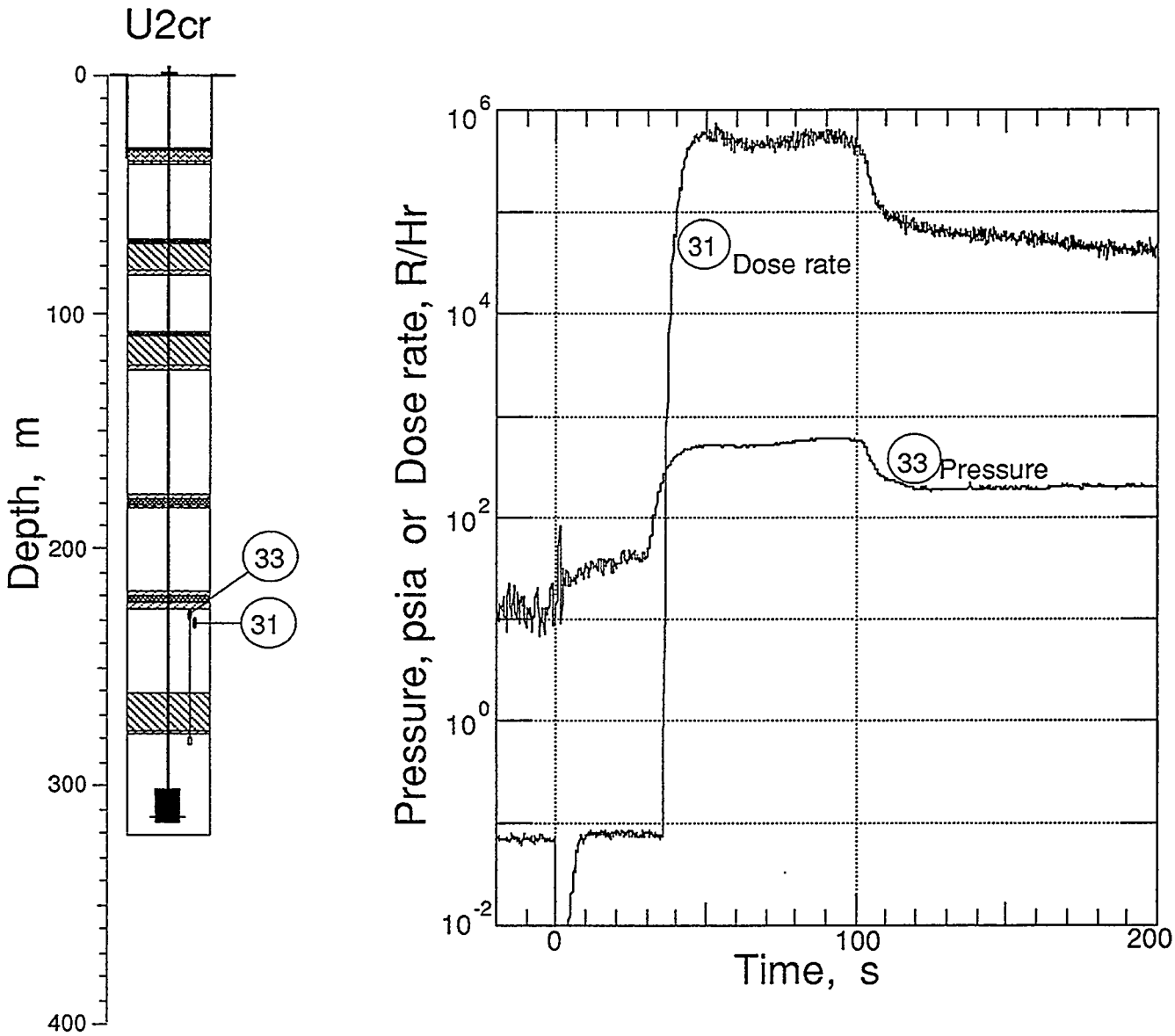

Figure 3.12 Comparison of the first 200 s of the radiation measured at station 31 with the gas pressure measured at station 33.

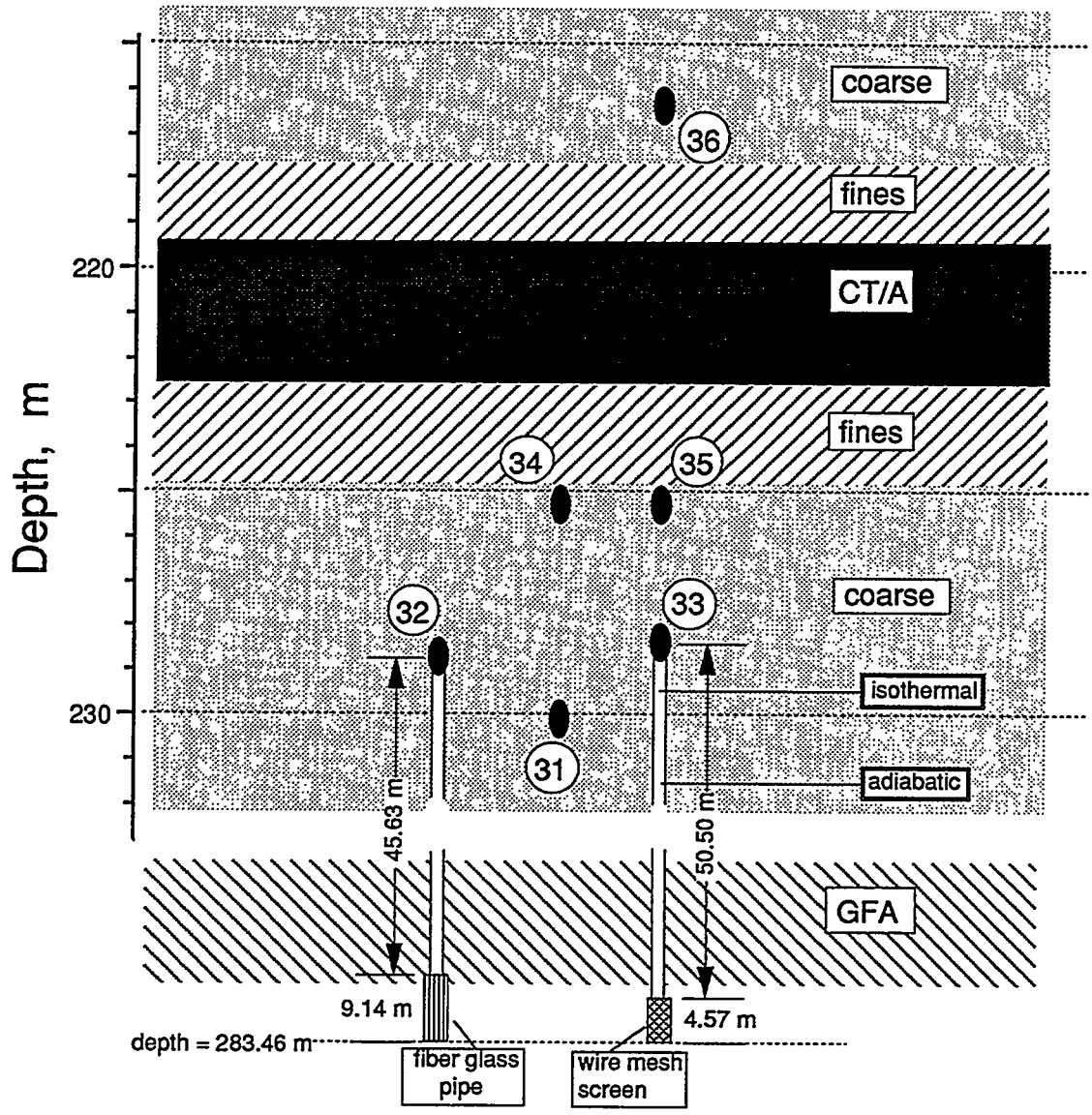

Figure 3.13 Sketch of the containment instrumentation in the region of gas seal CT/A plug 2. Pressure and radiation stations are represented by solid ellipses. Elevations between depths of 215 and 333 m are to scale while lateral dimensions are not to scale. Positions labeled by "adiabatic" and "isothermal" are those elevations to which the radioactive gas would rise under the pressure measured at station 33.

3.3 Motion

Explosion-induced motion histories measured on the WEXFORD event are shown in figures 3.15-3.19. Characteristics of the motion and of the motion transducers are given in tables 3.1–3.3.

The transducers at station 1 (on top of the emplacement pipe) were driven so far beyond their system limits that the accelerometer was not processed beyond being digitized. Velocimeter data are presented, but these are valid only at times greater than 0.2 s. The derived displacement history at station 1 (figure 3.17) is included only for completeness: it is not valid due to the lack of information during the first peak in velocity.

3.4 Collapse phenomena

Collapse motion histories are shown in figures 3.20-3.22. All motion stations below the top TPE plug (at the bottom of the surface casing) were lost at collapse between 1588 and 1597 s. All stations in and above the top plug survived collapse. Station 1 (figure 3.22) was mounted on the top of the emplacement pipe. Recording was terminated about 15 minutes after the first indication of collapse was detected and no collapse signals were captured at stations 61 (in the ground surface 15.2 m from SGZ) and at station 71 (in the recording trailer). In the ensuing days the small, off-center crater continued to grow until it encompassed the emplacement hole and took on a "cookie-cutter" appearance.

The CLIPER cable (station 91) performed as expected, giving the lower position of the cable end as a function of time during the cavity collapse. These data are shown in figure 3.23 along with selected wave forms of both pressure and motion (not to vertical scale). The emplacement pipe (station 1) begins its motion at about 1593 s, the time that the collapse reaches the second soft CT/A plug at a depth of 180 m, as shown in figure 3.23.

A vertical, linear array of seven proximity switches was mounted in the top SGC plug next to the bottom of the surface casing. Switch states labeled "on" imply the nearby presence of ferrous metal (surface casing) and "off"; its absence. Switch "a" was inoperative pre-shot and is not reported. No change of switch state was observed until the time of collapse (1596.3 s) when switches , "b", and "e" registered a change of state (switch "f" went into an indeterminate state at collapse time and, for clarity, is not reported). Figure 3.24 shows the switch closure history around collapse time. The proximity switch data suggest that the collapse drove the switch array greater than 5 cm into the casing. (The switches had a vertical separation of 5.08 cm. and the closure of switch "b" followed that of switch "e" by about 30 ms.)

The geophone and sensitive accelerometer data are shown in figure 3.25 to the maximum time of data recording. No activity was observed by either gauge after about 1630 s giving credence to the statement that the jump in the radiation output of station 39 (figure 3.9) at around 6000 s is likely due to a system instability.

Table 3.1 Summary of Motion

Gauge	Slant Range (m)	Arrival Time (ms)	Acceleration Peak (g)	Velocity Peak (m/s)	Displacement Peak (cm)	Displacement Residual (cm)
1av	316	75.3[a]	b	b	b	b
1uv	-	-	-	b	b	b
21av	199.2	47[a], 108	4.5[c]	0.84	17.7	7[d]
21uv	-	-	-	0.82	16.7	5.5
22av	238.2	58[a], 128	2.5	0.65	15.6	6.5[d]
22uv	-	-	-	0.57	13.0	3.0
61av	315	186	2.25	0.85	13.2	5.0
61uv	-	-	-	0.83	13.4	5.0
71av	386[d]	215	1.4	0.75	8.5	-1.5[d]
71uv	-	-	-	0.72	7.8	-3.0[d]

(a) Pipe-induced motion.
(b) Out of band.
(c) Possibly out of band.
(d) Approximate.

Table 3.2 Accelerometer Characteristics

Gauge	Natural Frequency (Hz)	Damping Ratio	System Range (g's)
1av	580	0.62	±30
21av	200	0.73	±8
22av	280	0.64	±7
61av	240	0.77	±20
71av	240	0.75	±10

Table 3.3 Velocimeter Characteristics

Gauge	Natural Frequency (Hz)	Time to 0.5 Amplitude (s)	Calibration Temperature (°C)	Operate Temperature (°C)	System Range (m/s)
1uv	3.622	8.63	24.24	23.14	±12
21uv	3.567	9.82	23.82	44.85	±6
22uv	3.454	10.92	23.45	40.17	±8
61uv	3.778	7.43	22.75	27.63	±8
71uv	3.253	11.75	24.27	26.17	±4

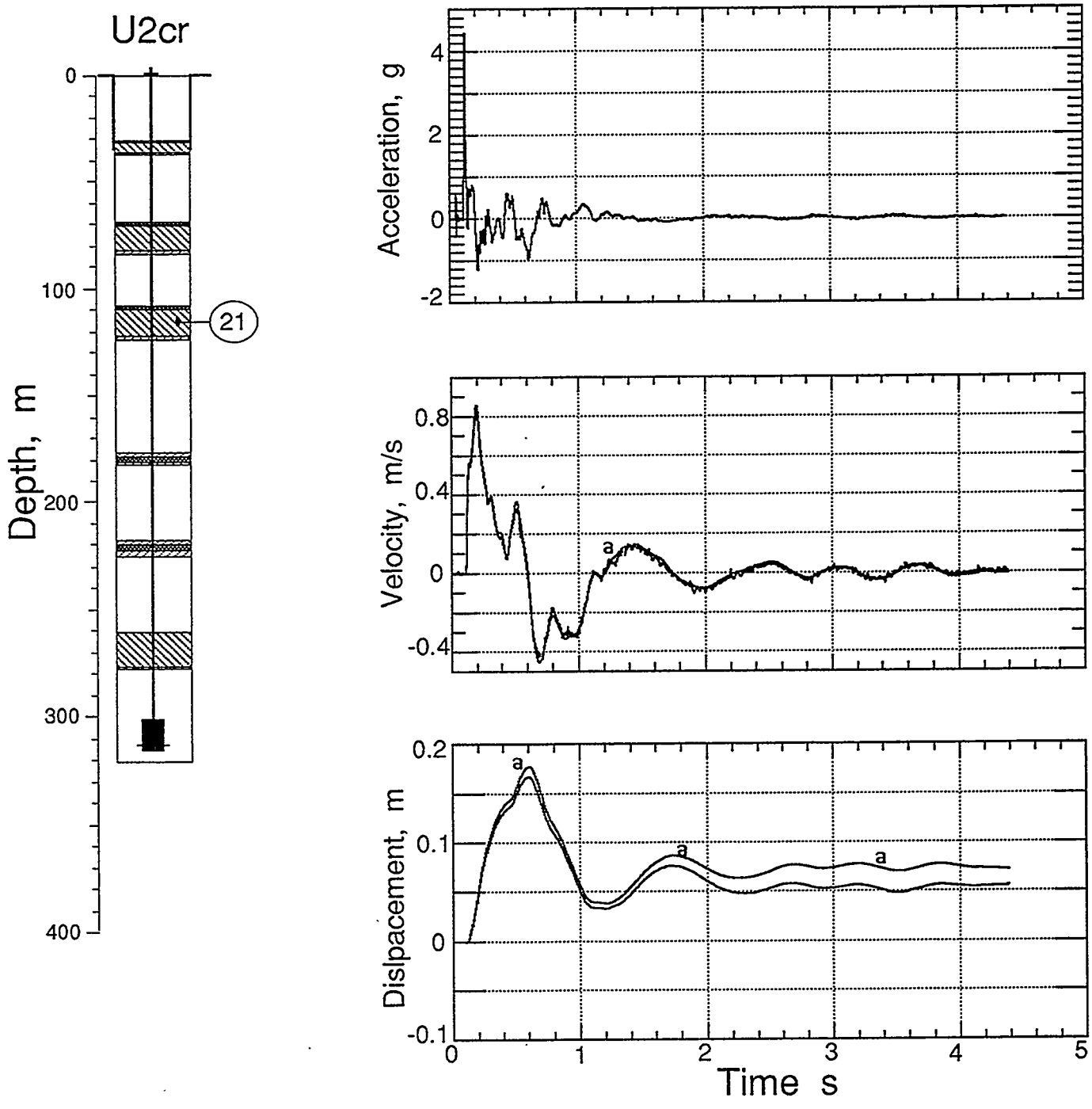

Figure 3.15 Explosion-induced vertical motion of GFA plug 4 (station 21 at a depth of 115.8 m). Traces annotated with "a" are derived from the accelerometer.

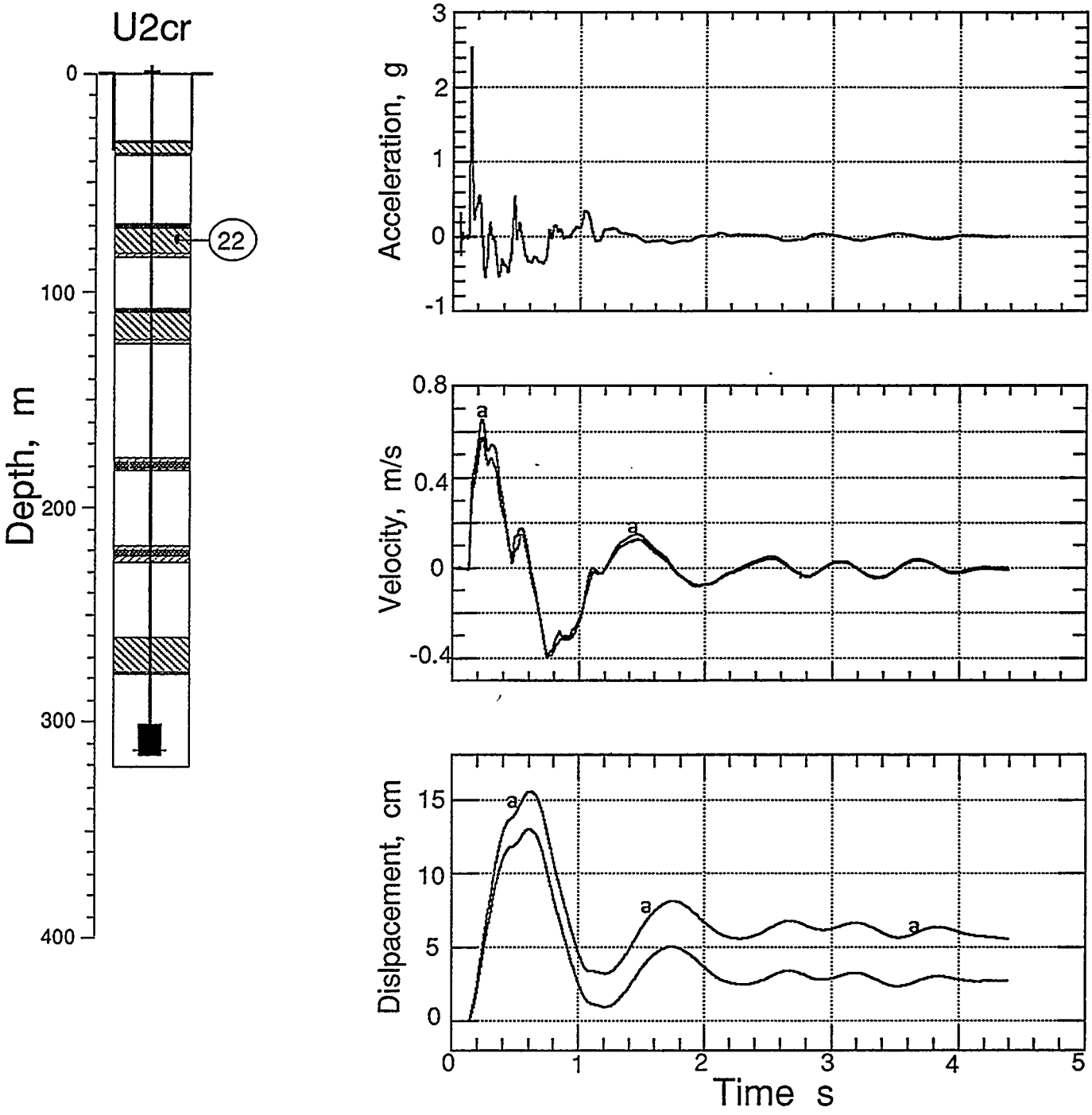

Figure 3.16 Explosion-induced vertical motion of GFA plug 5 (station 22 at a depth of 76.2 m). Traces annotated with "a" are derived from the accelerometer.

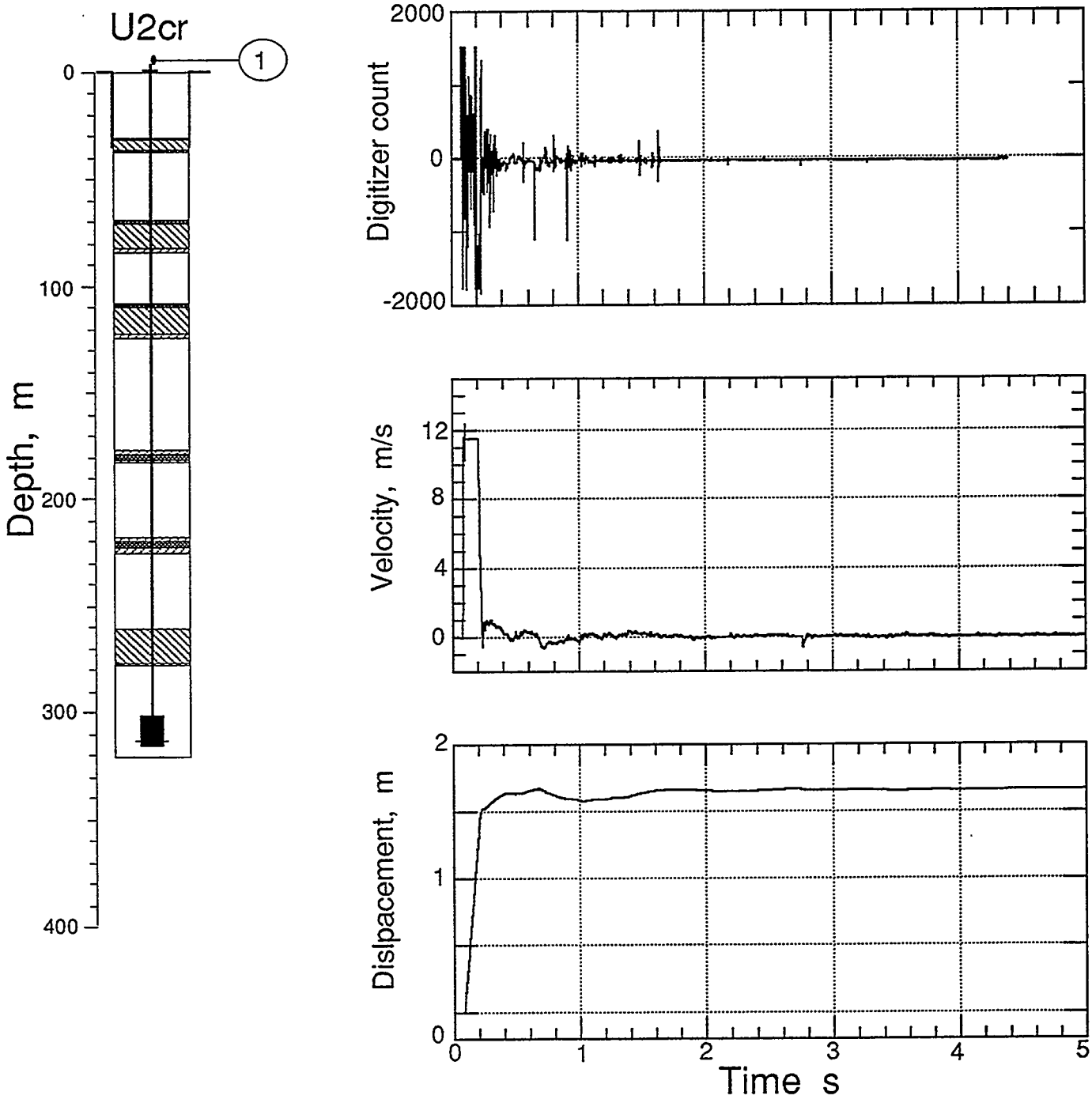

Figure 3.17 Explosion-induced vertical motion of the top of the emplacement pipe (station 1).

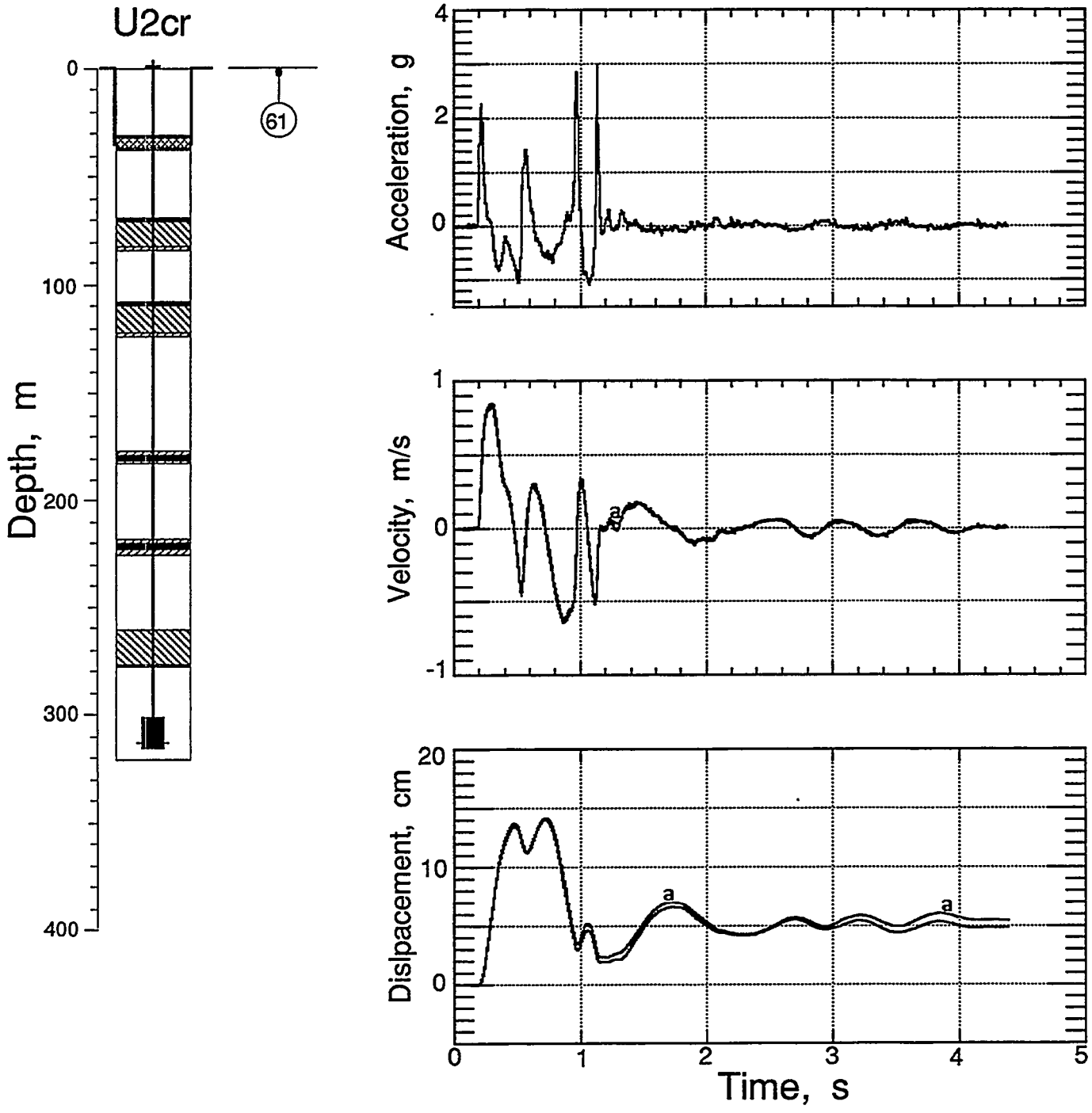

Figure 3.18 Explosion-induced vertical motion of the ground surface (station 61 at a horizontal range of 15.24 m and a depth of 0.9 m). Traces annotated with "a" are derived from the accelerometer.

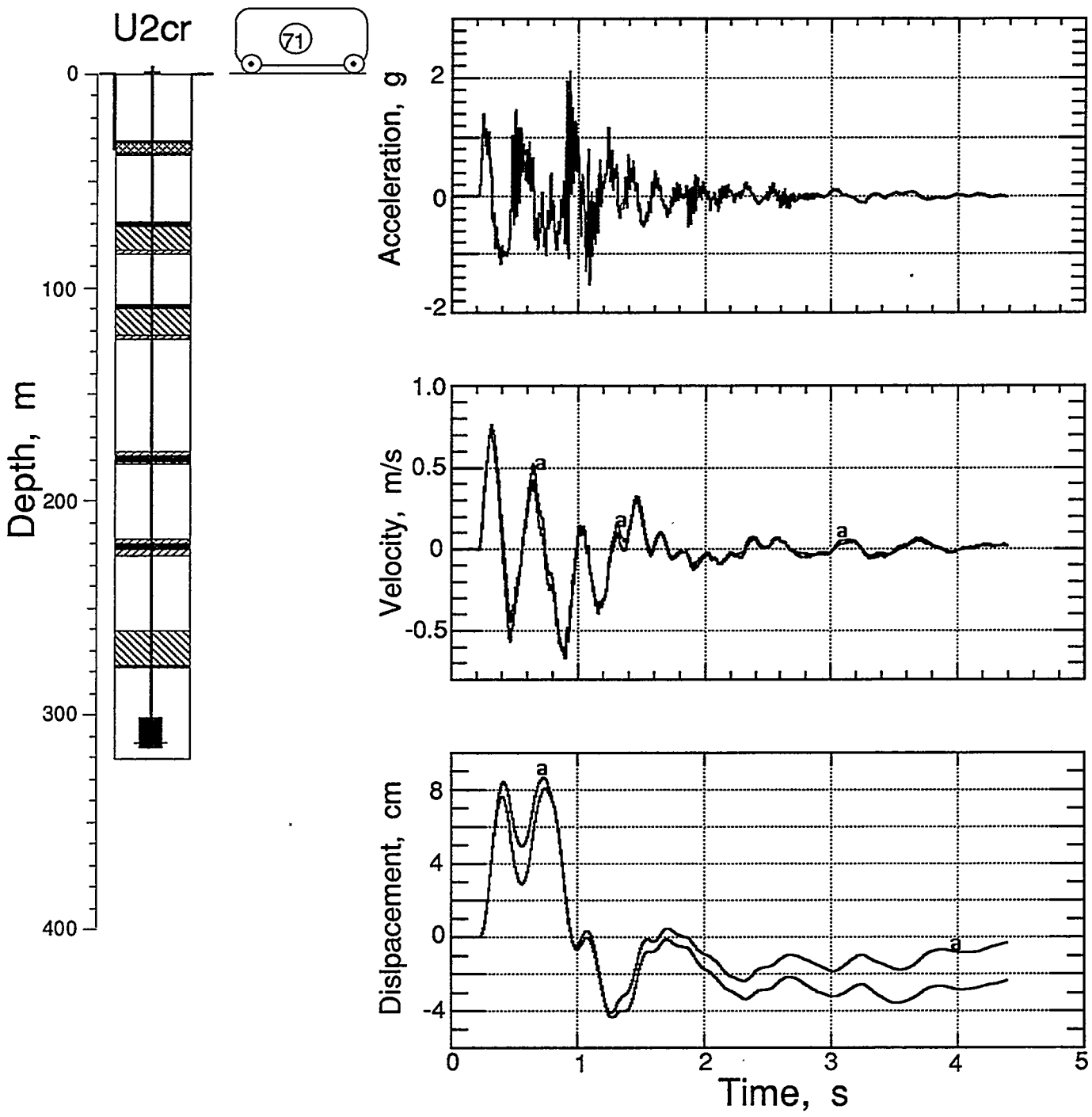

Figure 3.19 Explosion-induced vertical motion of the recording trailer (station 71 at a horizontal range of about 386 m). Traces annotated with "a" are derived from the accelerometer.

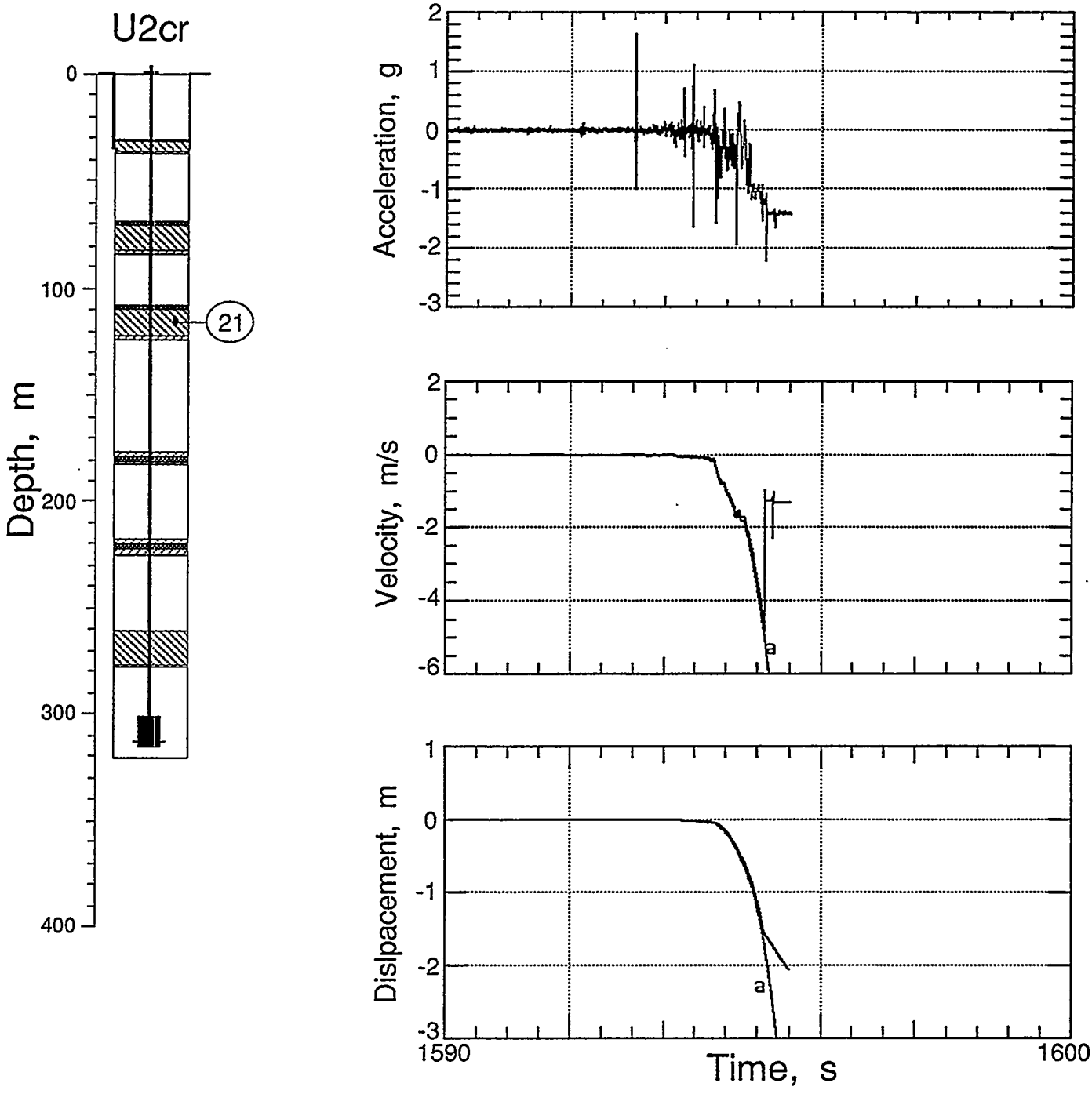

Figure 3.20 Collapse-induced vertical motion of GFA plug 4 (station 21 at a depth of 115.8 m). Traces annotated with "a" are derived from the accelerometer. Signal was lost at about 1595.1 s.

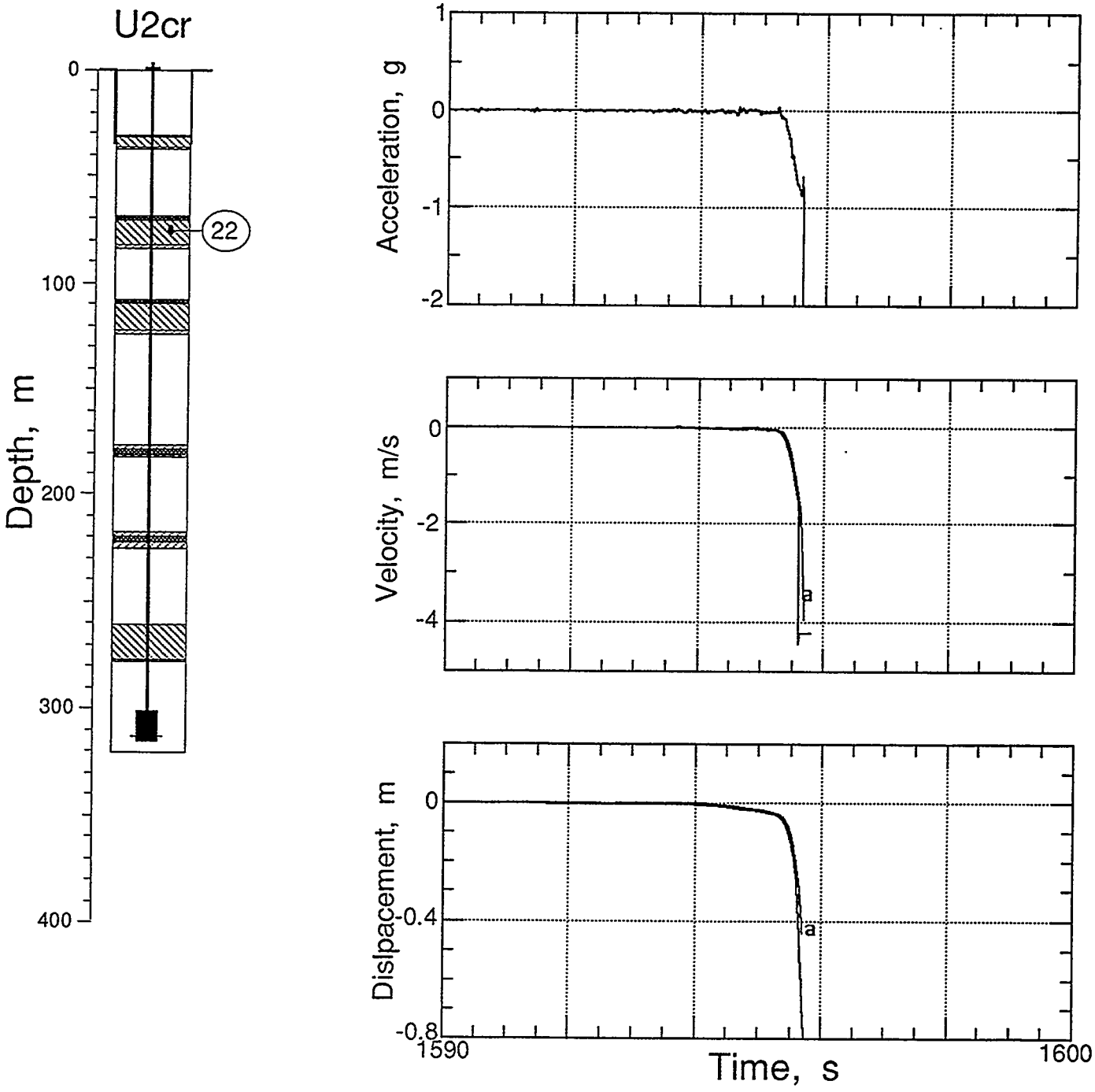

Figure 3.21 Collapse-induced vertical motion of GFA plug 5 (station 22 at a depth of 76.2 m). Traces annotated with "a" are derived from the accelerometer. Signal was lost at about 1595.6 s.

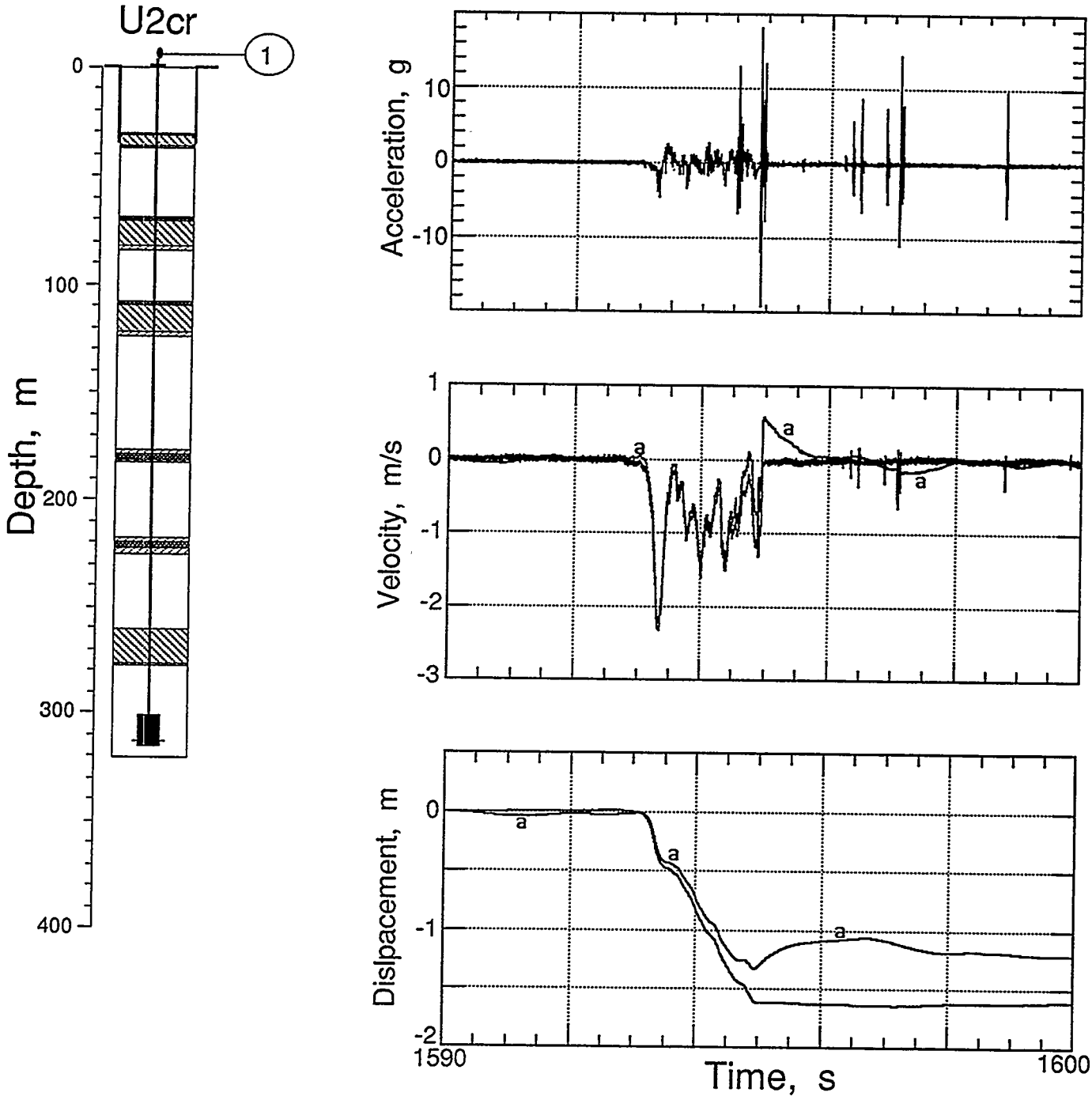

Figure 3.22 Collapse-induced vertical motion of the top of the emplacement pipe (station 1). Signals from this station were not lost during the recorded collapse motion.

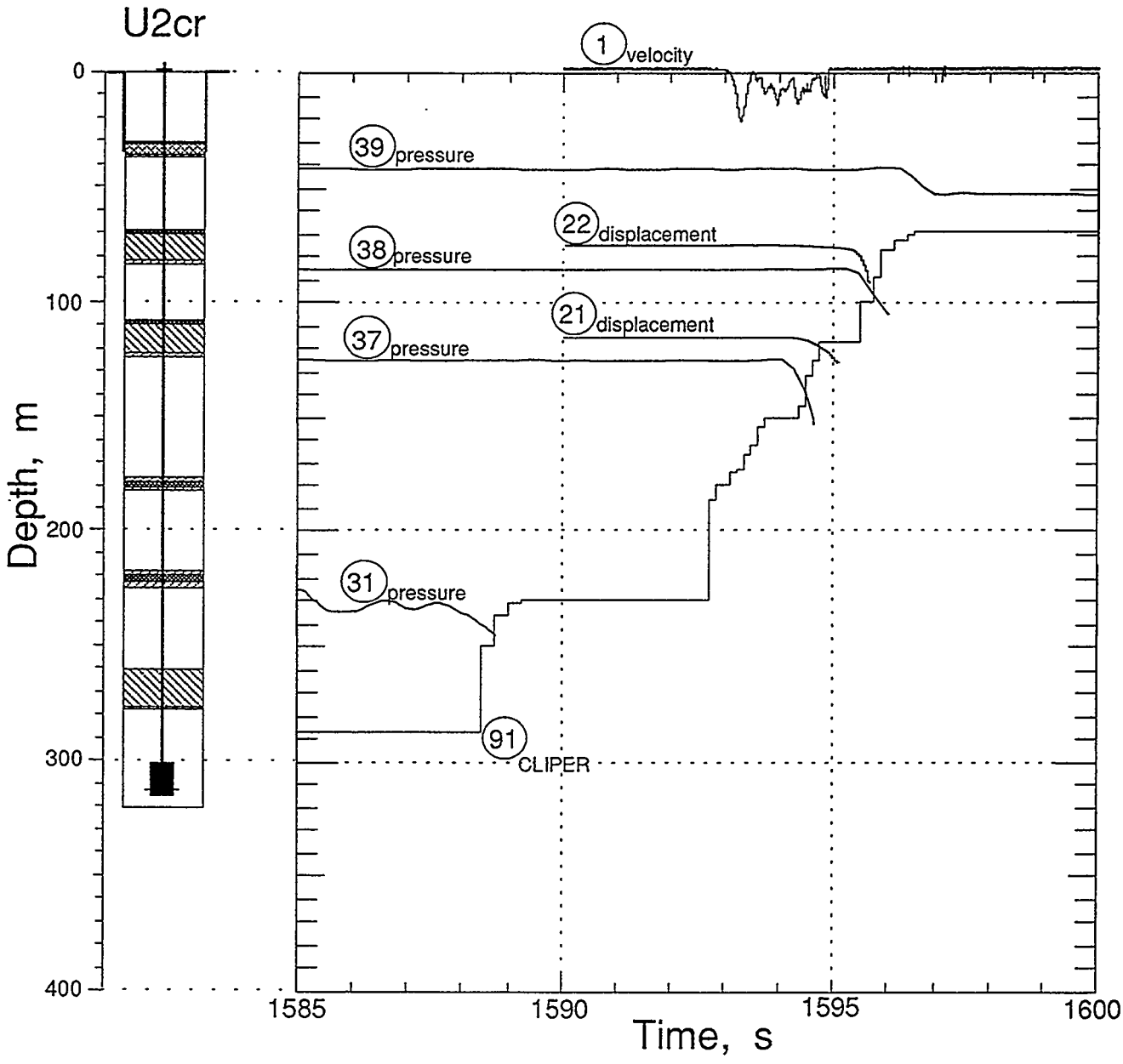

Figure 3.23 Progression of collapse as determined from the CLIPER (station 91) and various pressure and motion records in the emplacement hole. Note that the emplacement pipe (station 1) begins dropping when the collapse, as determined from station 91, reaches a depth of about 180 m.

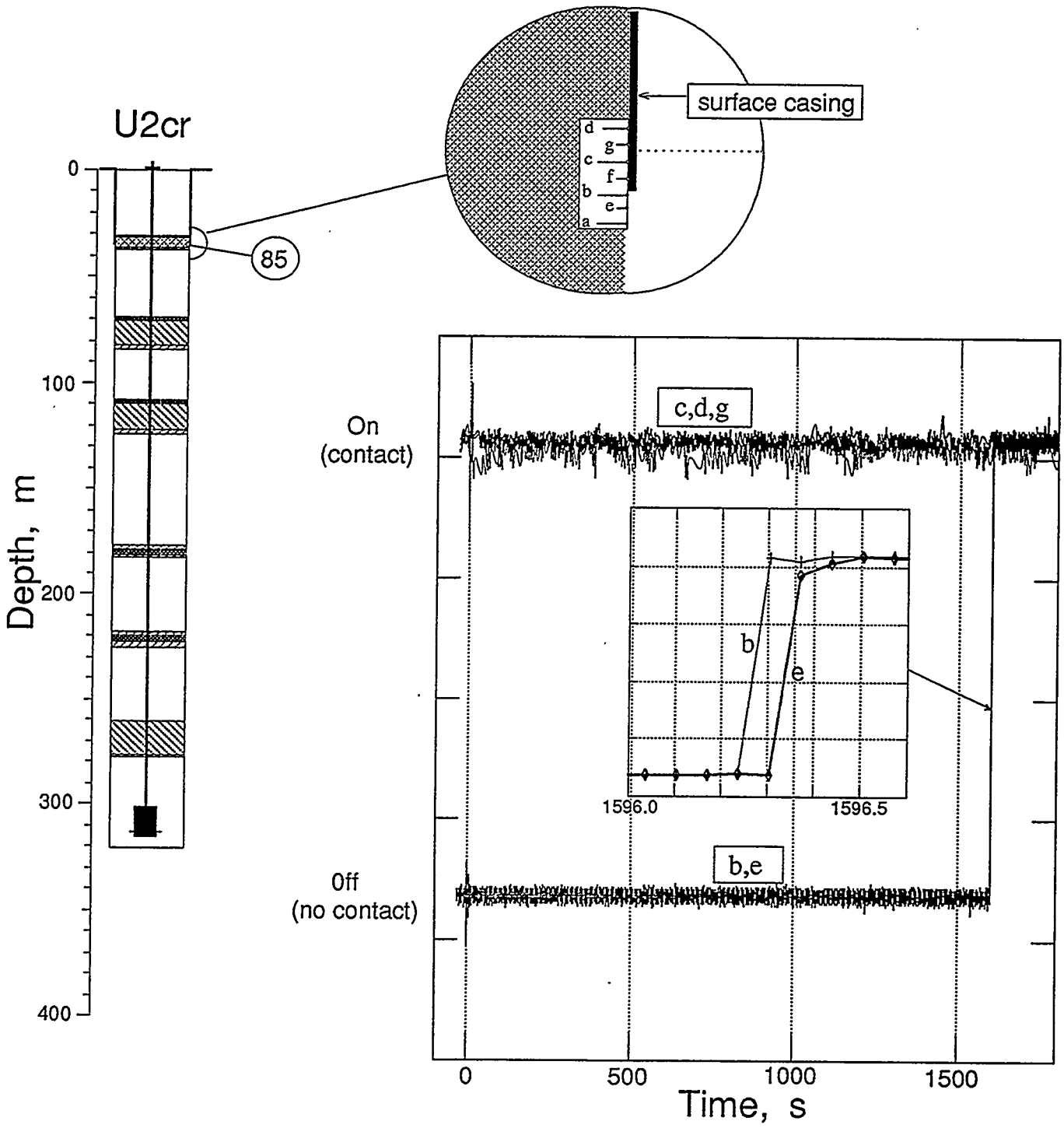

Figure 3.24 Output of linear array of proximity switches in the top TPE plug at the bottom of the emplacement pipe. Only switches "b" and "e" changed state at collapse time. See insert within time history wherein markers denote each of the sampled data points.

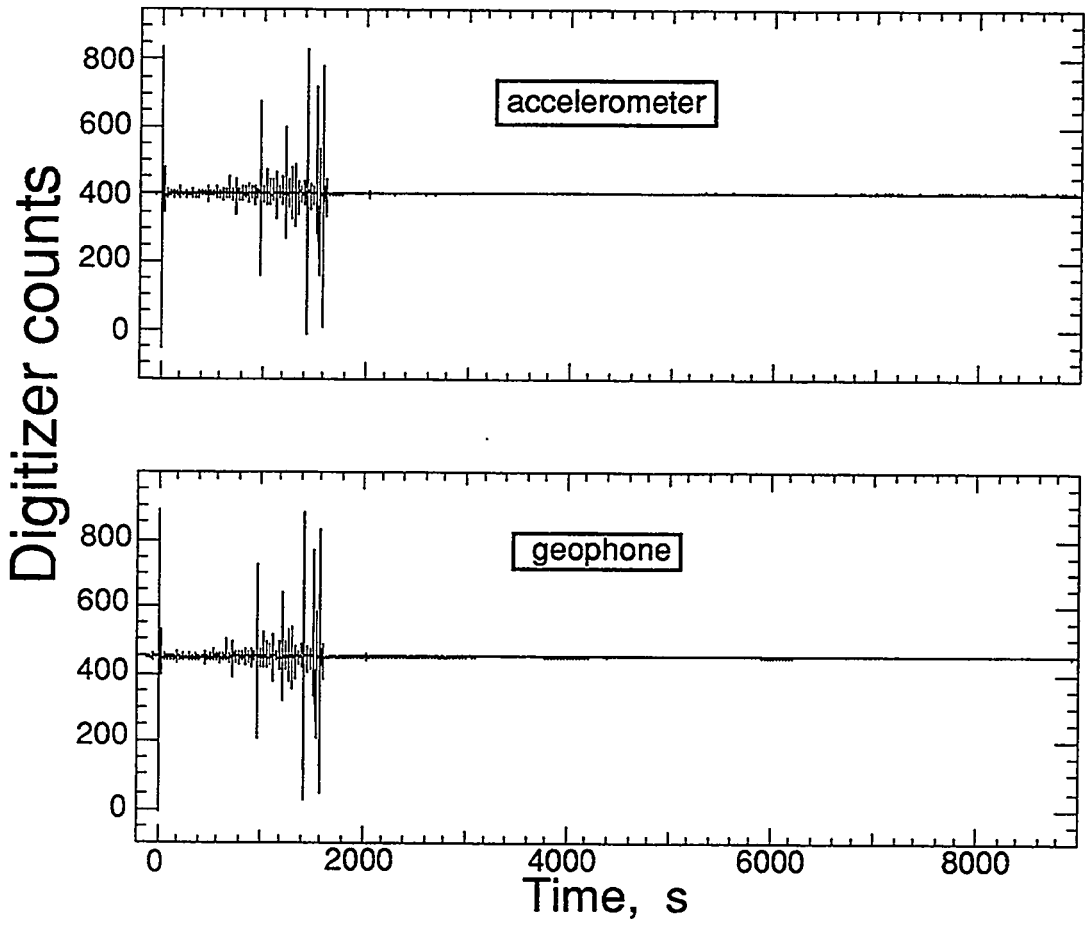

Figure 3.25 Histories of the geophone and sensitive accelerometer placed in the ground surface near the recording trailer (station 62). Note that all sensed activity ended shortly after 1600 s.

4. Other Measurements

4.1 Stress and strain in the deepest plugs

A set of four bi-axial stress and strain transducers were fielded in the deepest GFA plug to test the performance of a new fluid-coupled flat pack system[7]. The transducers consist of a planar grid of Ytterbium as the stress sensing element. Since Yb is sensitive to strain as well as stress, a Constantan grid was interwoven with the Yb grid to sense only strain. Each of the transducers consisted of a pair of planar grids oriented to sense both radial and transverse (vector) components of stress and strain.

Time histories of the stress and strain are shown in figures 4.1, 4.3, 4.5 and 4.7. Note that there is a common wave form in all records starting at zero time and lasting for about 30 ms. It is postulated that the EMP coupled to the element grid and associated electronics: no data prior to 30 ms after zero time should be taken as stress or strain information.

Strain is removed from the Yb output records as follows. The Yb output includes contributions from both stress and strain, while the Constantan output is produced by strain only. Let ε denote strain, σ denote stress, C Constantan, and Y Ytterbium. A gauge output is given by:

$$\left.\frac{\Delta R}{R}\right|_{Y} = \left.\frac{\Delta R}{R}\right|_{Y,\sigma} + \left.\frac{\Delta R}{R}\right|_{Y,\varepsilon} = \left.\frac{\Delta R}{R}\right|_{Y,\sigma} + G_Y * \varepsilon$$

The gauge strain factors are $G_Y = -3.3$ and $G_C = 2.1$ for Yb and Constantan, respectively. Combining these with the above equation and noting that $\left.\frac{\Delta R}{R}\right|_{C,\sigma} = 0$

gives:
$$\left.\frac{\Delta R}{R}\right|_{\sigma} = \left.\frac{\Delta R}{R}\right|_{Y} + 1.57 * \left.\frac{\Delta R}{R}\right|_{C}$$

The time histories shown in figures 4.2, 4.4, 4.6 and 4.8 are the Ytterbium outputs with the strain component removed.

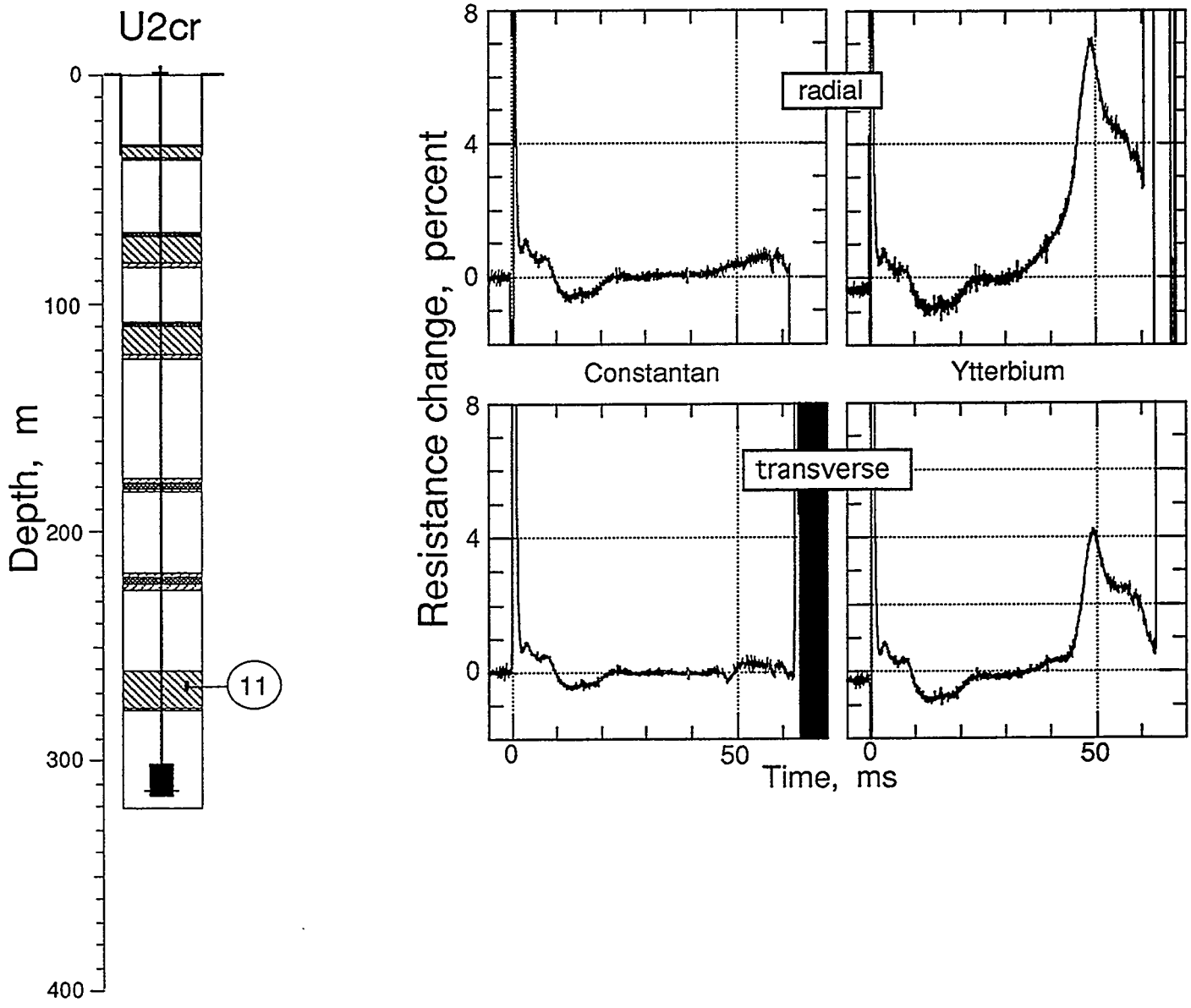

Figure 4.1 Bi-axial stress and strain in the deepest GFA plug at a depth of 267.31 m (station 11). Ytterbium data are NOT corrected for strain.

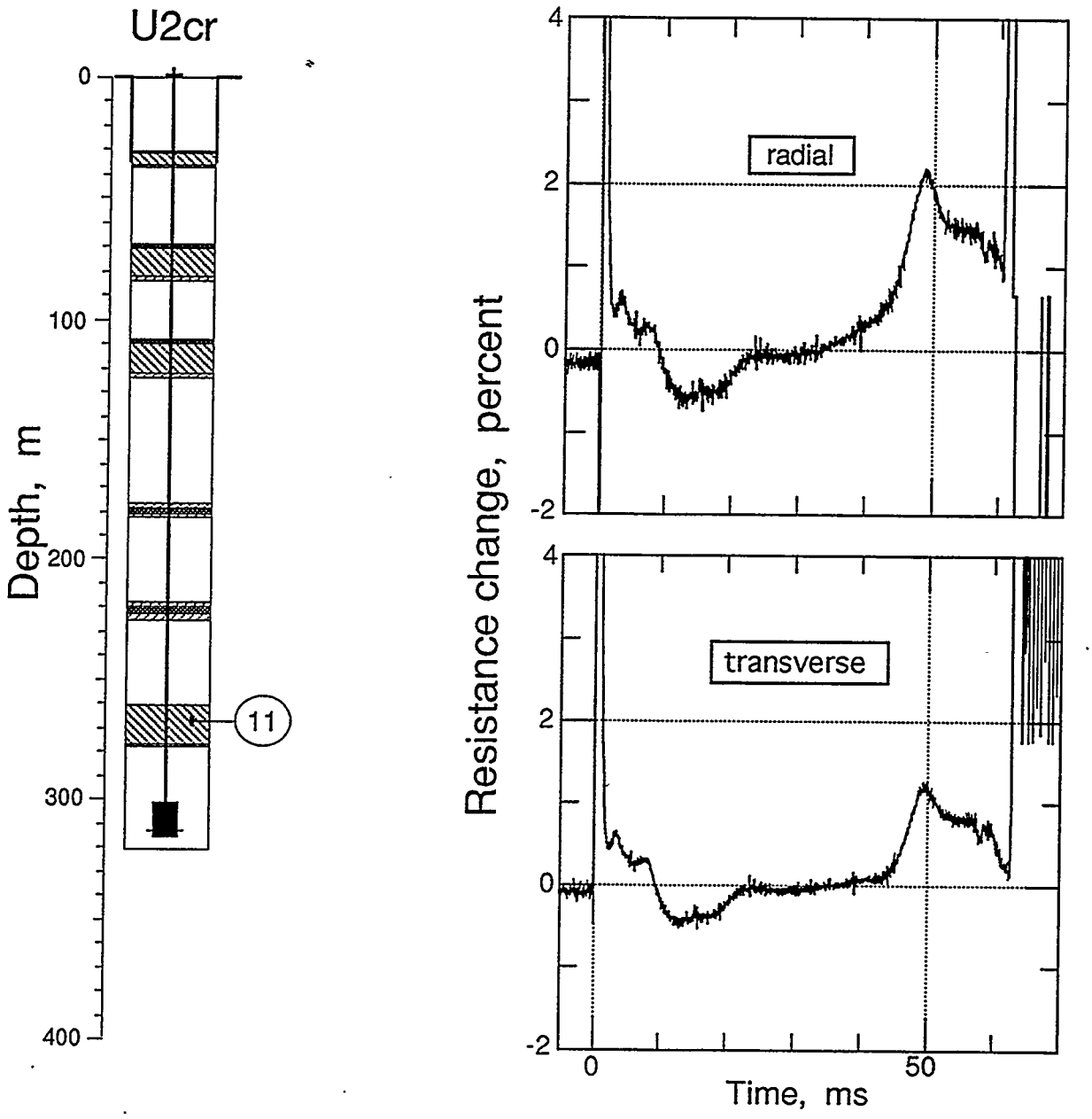

Figure 4.2 Bi-axial stress in the deepest GFA plug at a depth of 267.31 m (station 11), corrected for strain.

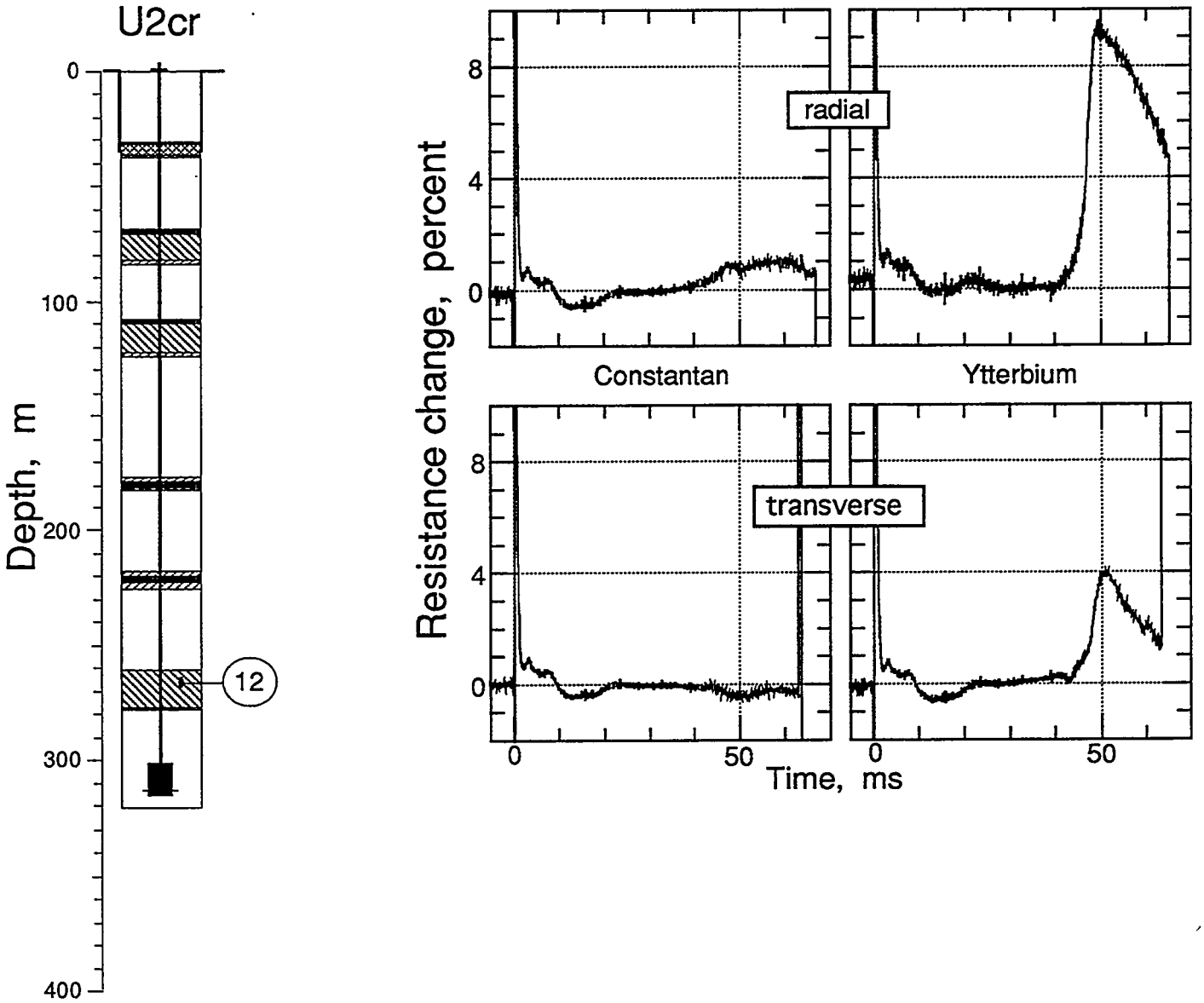

Figure 4.3 Bi-axial stress and strain in the deepest GFA plug at a depth of 267.31 m (station 12). Ytterbium data are NOT corrected for strain.

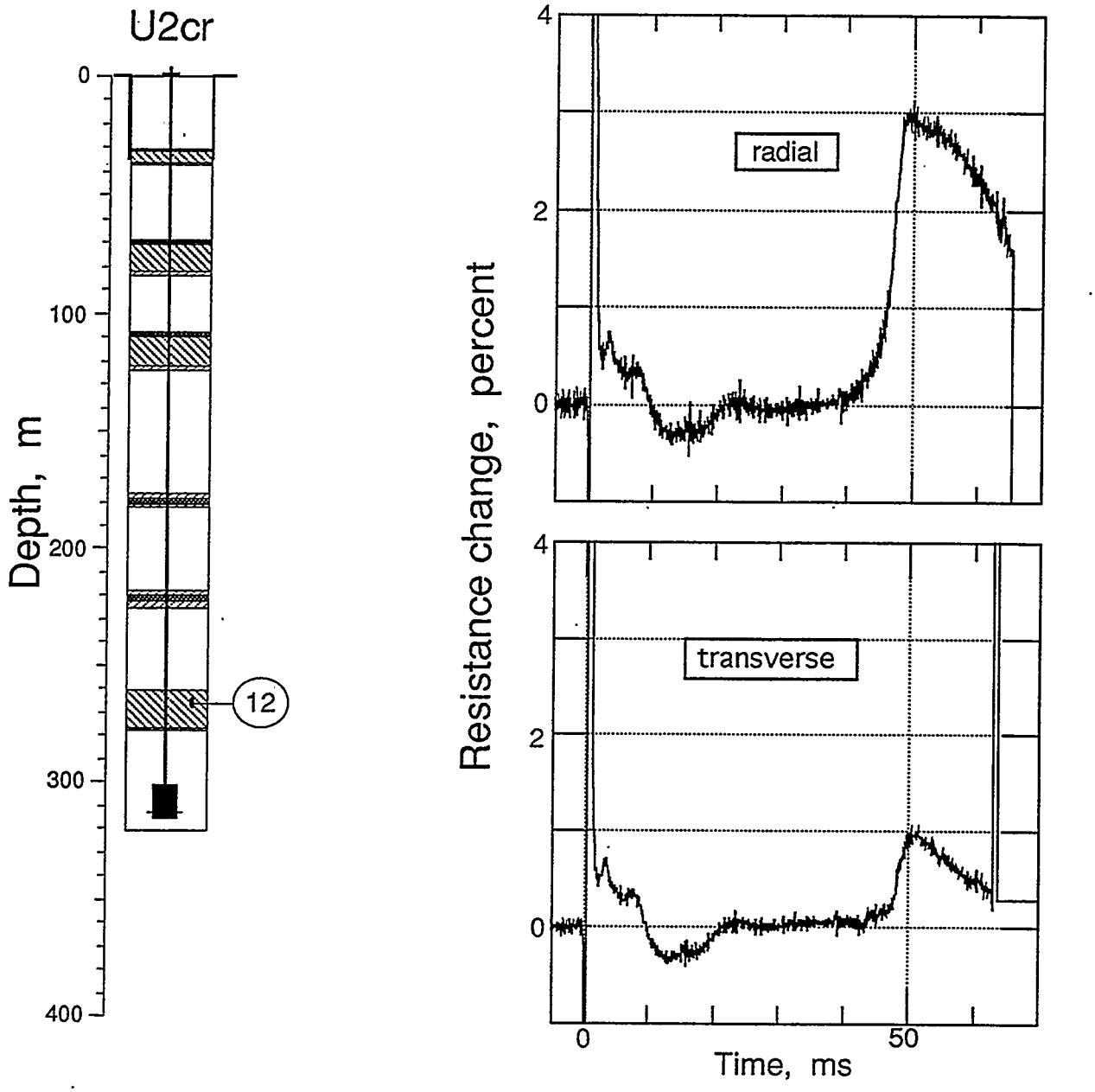

Figure 4.4 Bi-axial stress in the deepest GFA plug at a depth of 267.31m (station 12), corrected for strain.

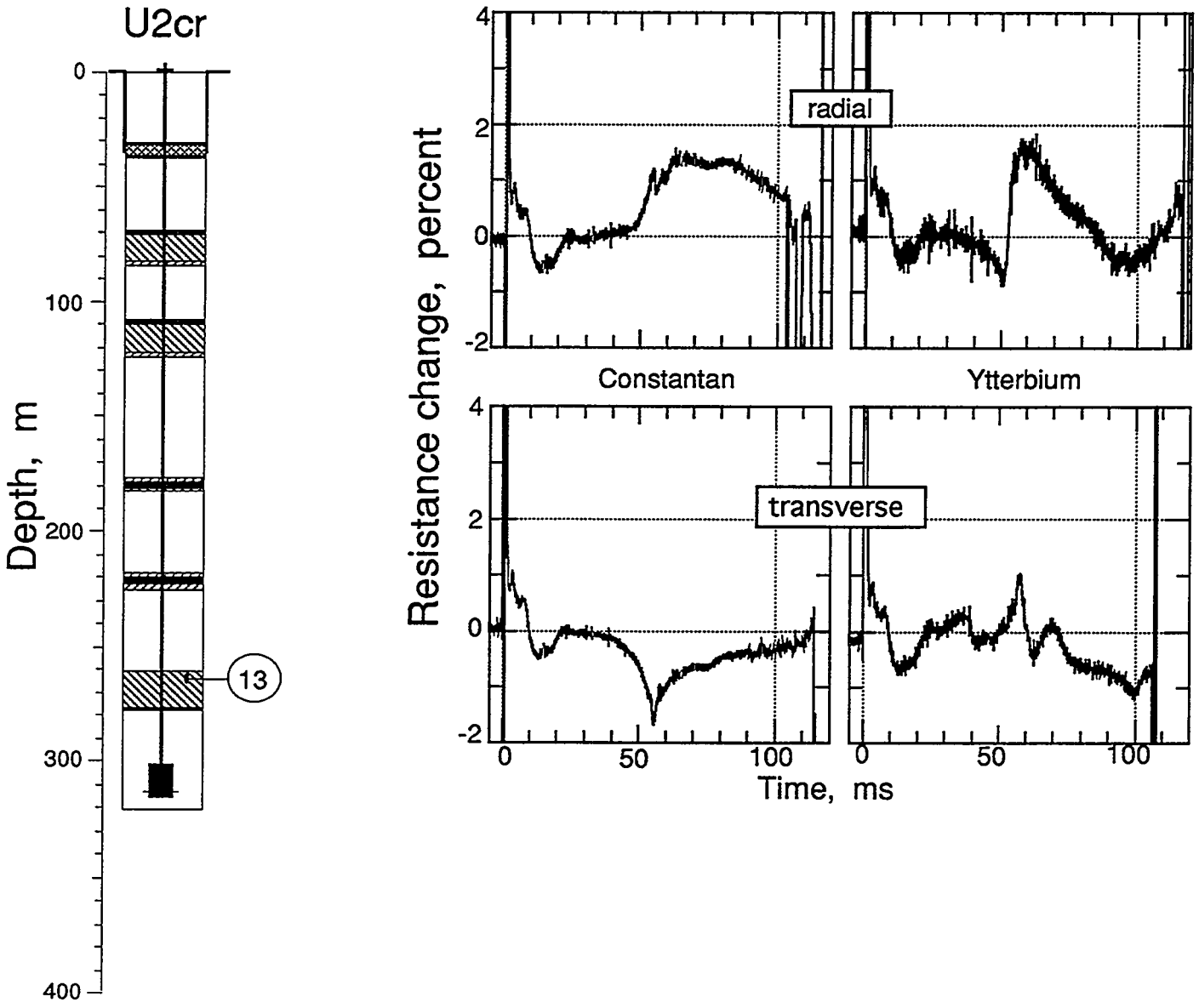

Figure 4.5 Bi-axial stress and strain in the deepest GFA plug at a depth of 263.65 m (station 13). Ytterbium data are NOT corrected for strain

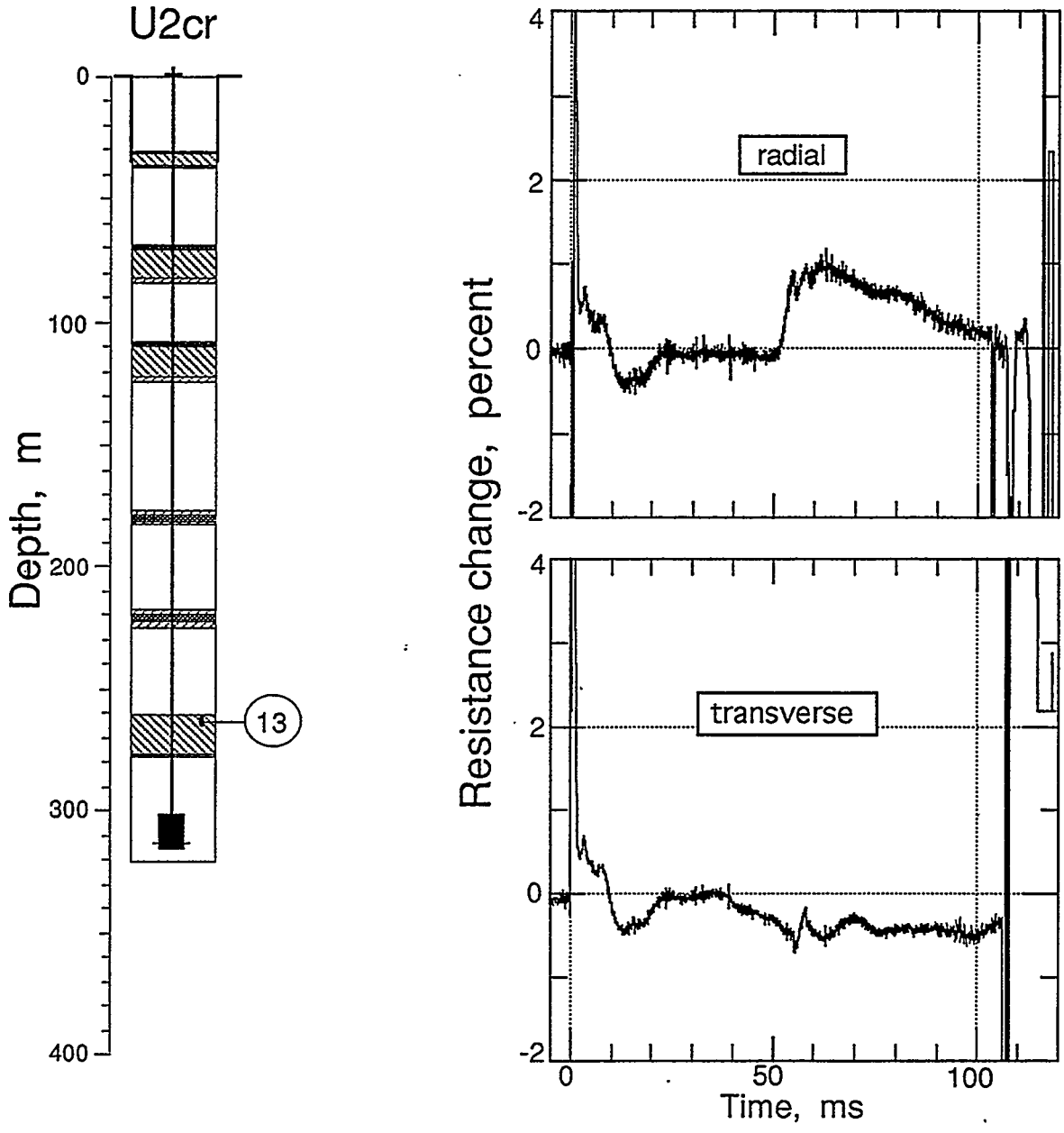

Figure 4.6 Bi-axial stress in the deepest GFA plug at a depth of 263.65 m (station 13), corrected for strain.

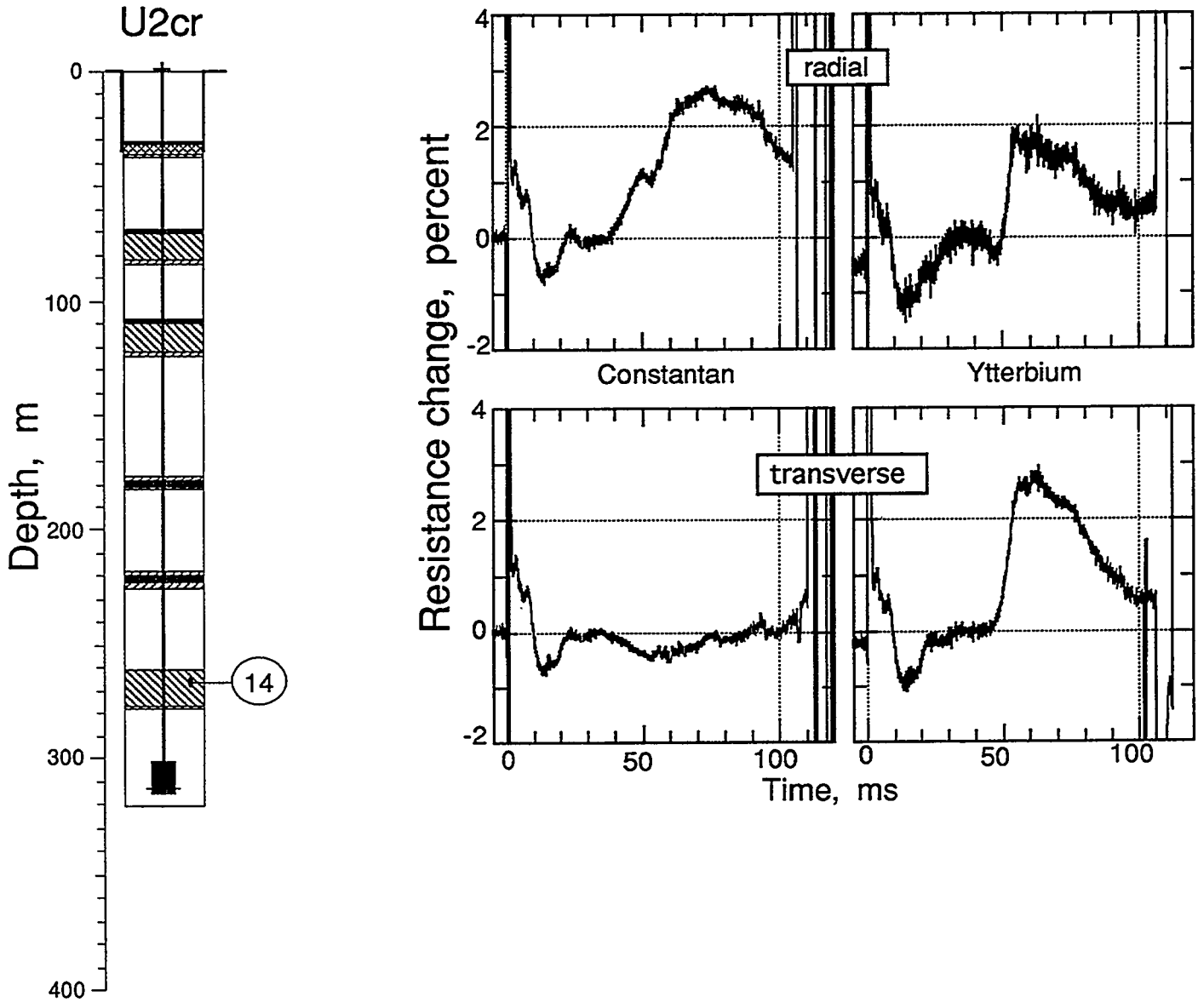

Figure 4.7 Bi-axial stress and strain in the deepest GFA plug at a depth of 263.65 m (station 14). Stress data are NOT corrected for strain.

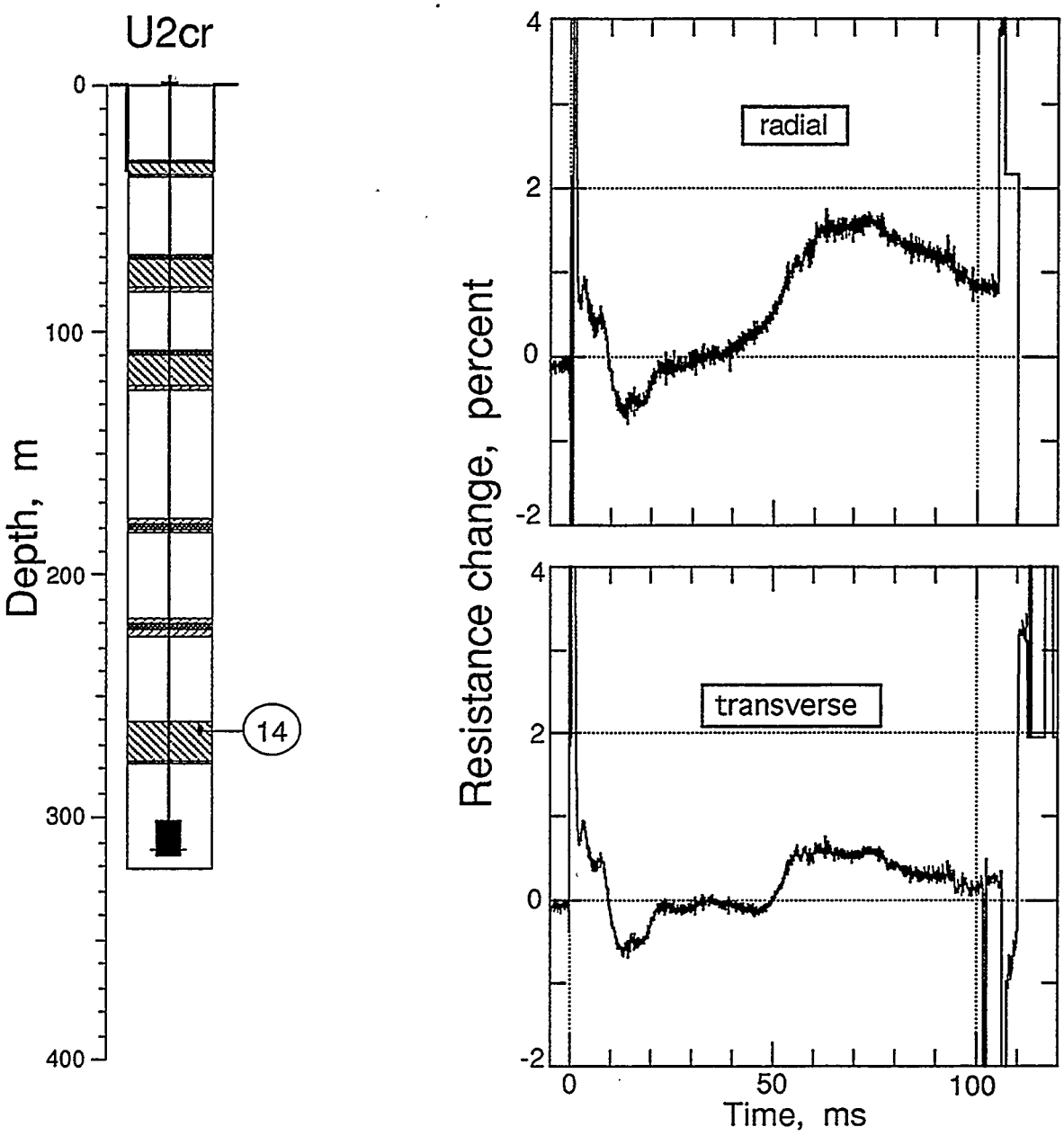

Figure 4.8 Bi-axial stress in the deepest GFA plug at a depth of 263.65 m (station 14), corrected for strain.

References

1. J. L. Wagoner, "U2cr Site Characteristics Report," CP 84-24, Lawrence Livermore National Laboratory, Livermore, CA, March 16, 1984.

2. Alfred E. Burer, "Containment Report for U2cr," Holmes & Narver, NTS:A2:84-76, August 28, 1984.

3. LLNL contacts for additional information: H. Goldwire and R. E. Heinle (CORTEX and SLIFER data)

4. B. William Bellow, "Special Measurements Final Engineering Report WEXFORD, U2cr", EG&G, Energy Measurements, Las Vegas, NV, SM:85E-120-22, 1 October, 1984.

5. B. William Bellow, "Special Measurements Physics/Instrumentation for WEXFORD, U2cr, Revision 'A'", EG&G, Energy Measurements, Las Vegas, NV, SM:84E-120-October,1984.

6. C. Cordill, "WEXFORD, U2cr, Emplacement Pipe Load History", Lawrence Livermore National Laboratory, Internal memo CG-84-191, October 31, 1984

7. J. Kalinowski, T. Stubbs, L. Davies, and B. Hudson, "Recent stress gage developments", Range Commanders Council, Telemetry Group, 4-6 July, 1985, Monterey, California.

Distribution:

LLNL

TID (11)	L-053
Test Program Library	L-045
Containment Vault	L-221
Burkhard, N.	L-221
Cooper, W.	L-049
Denny, M.	L-205
Goldwire, H.	L-221
Heinle, R. (5)	L-221
Mara, G.	L-049
Moran, M. T.	L-777
Moss, W.	L-200
Patton, H,	L-205
Pawloski, G.	L-221
Rambo, J.	L-200
Roth, B.	L-049
Valk, T.	L-154
Younker, L.	L-203

LANL

App, F.	F-659
Brunish, W.	F-659
Kunkle, T.	F-665
Trent, B.	F-664

Sandia

Chabai, A.	MS-1159
Smith, Carl W.	MS-1159

EG&G/AVO

Brown, T.	A-5
Gilmore, L.	A-1
Hatch, M.	A-5
Still, G.	A-5
Stubbs, T.	A-5

EG&G/NVO

Bellow, B.	N 13-20
Davies, L.	N 13-20
Moeller, A.	N 13-20
Robinson, R.	N 13-20
Webb, W.	N 13-20

DNA

Ristvet, B.

S-Cubed

Peterson, E.

Eastman Cherrington Environment
1640 Old Pecos Trail, Suite H
Santa Fe, NM 87504

Keller, C.